



# Review on the Phase Equilibria in Iron Ore Sinters

Eetu-Pekka HEIKKINEN, Mikko ILJANA and Timo FABRITIUS\*

Process Metallurgy Research Unit, PO Box 4300, University of Oulu, FI-90014 Finland.

(Received on April 15, 2020; accepted on July 29, 2020)

Sintering process is a commonly used pre-treatment process for iron containing burden materials with an aim to produce porous, agglomerated sinter material with suitable properties to be charged into the blast furnace. During the sintering process the material undergoes a series of reactions, during which the conditions vary considerably. These changes in temperature and state of oxidation cause changes in the mineralogical composition of the material and although the sintering process does not completely reach the chemical equilibrium, it is important to understand the phase equilibria of the sinter system in order to analyse and control the effect of various factors on the sintering process.

The purpose of this paper is to give a review on the research related to phase equilibria in iron ore sinters. The main components of the sinter are FeO, Fe<sub>2</sub>O<sub>3</sub>, SiO<sub>2</sub>, CaO, Al<sub>2</sub>O<sub>3</sub> and MgO and by studying the phase equilibria of this system, the behaviour of sinters can be evaluated. Based on the experimental data, oxide databases have been created to provide thermochemical data of all the necessary compounds within this system. Concerning the solutions, more research is required related to SFCA phases. These databases are commercially available with thermochemistry software and can be used to compute phase diagrams illustrating the effect of different factors on the phase equilibria within the FeO–Fe<sub>2</sub>O<sub>3</sub>–SiO<sub>2</sub>–CaO–Al<sub>2</sub>O<sub>3</sub>–MgO system. Phase diagrams provide a useful tool to study the behaviour of the material in both sintering process itself as well as in the following reduction processes such as the blast furnace.

KEY WORDS: agglomeration; sintering; sinter; iron ore; ironmaking; phase equilibria.

## 1. Introduction

Sintering is a thermal agglomeration process that is applied to a mixture of iron ore fines, recycled ironmaking by-products, fluxes, slag-forming agents, and solid fuel (coke).<sup>1–4</sup> In the sintering process the sinter mixture undergoes a series of reactions,<sup>2,4,5</sup> during which the process temperature rises up to 1 300–1 480°C<sup>4</sup> or to 1 300–1 375°C<sup>5</sup> at maximum. The purpose of the sintering process is manufacturing a porous product with suitable thermal, mechanical, physical and chemical characteristics to be used as blast furnace feed to produce hot metal.<sup>1–3</sup> The bonding between the particles is caused by partial melting and recrystallization, and therefore no additional binder needs to be added in this process.<sup>4</sup> Sinter performs well in the blast furnace, particularly if it is made with fluxes added before sintering and is sized to 25 mm × 6 mm before charging into the furnace.<sup>6</sup> Sinter burdens in a blast furnace process are prevalent in European<sup>7</sup> and Asian<sup>7,8</sup> blast furnaces, while pellet burdens are used more commonly in Scandinavia and North America.<sup>7</sup> Both the sintering process and the sinter material have been widely studied in the iron and steelmaking industry as reported by *e.g.* Fernández-González *et al.*<sup>1–3,9</sup> in their recent review papers.

The sintering in iron and steel industry is most commonly implemented on a belt furnace, which can be divided into four different sections: cold and wet zone (below 100°C); drying zone (100–500°C); reaction zone (up to 1 300–1 480°C); and cooling zone. The cold and wet zone is formed by the mix to be sintered. The vaporisation of the moisture and subsequent dehydration of hydroxides take place in the drying zone. The main reactions occur in the reaction zone and those are: coke combustion (exothermal); decomposition of carbonates (endothermal); solid phase reactions; reduction of iron oxides; re-oxidation of iron oxides; and formation of the sintered mass. Cooling and re-crystallization of the sintered product take place in the cooling zone.<sup>2</sup> As material proceeds in the sintering belt, it gradually undergoes all these stages in such a way that all the above mentioned zones can be identified on a cross-section of the material on a certain location in the belt. The goal is to have material thoroughly sintered at the end of the belt.

The sintering process is very short and the conditions in the different parts of the sintering bed differ particularly with respect to the temperature and partial pressure of oxygen.<sup>6</sup> Hence, the mineral composition of sinter is not in a state of equilibrium, and there is a large variation in mineralogy between different sinter pieces. In addition, part of the minerals of the sinter mixture remain almost totally unchanged

\* Corresponding author: E-mail: [timo.fabritius@oulu.fi](mailto:timo.fabritius@oulu.fi)



throughout the whole sintering process. Such minerals are the coarsest magnetite and hematite grains and often the quartz and olivine grains.<sup>10)</sup> Despite the non-equilibrium and inhomogeneous nature of the sintering process, it is nevertheless important to understand the phase equilibria of the sinter system in order to analyse and control the effect of various factors (such as temperature, composition and state of oxidation) on the sintering process.<sup>11)</sup> The purpose of this paper is to give a review on the research related to phase equilibria in iron ore sinters with the main focus on the assessment of thermochemical data needed to model sinter system.

## 2. Iron Ore Sinter

Sinter is a very heterogeneous material and its properties vary considerably depending on the type of raw materials and blend. Usually the raw material blend consists of iron ore fines (with either hematite,  $\text{Fe}_2\text{O}_3$ , or magnetite,  $\text{Fe}_3\text{O}_4$ , as the main component), other iron containing fine materials (such as steelmaking dusts), slag forming substances (such as limestone, serpentine or silica sand), and fuels (coke breeze).<sup>1,10,12)</sup> Although iron oxide is the dominant component, sinters are commonly classified based on the amounts of other components. For example, Geerdes *et al.*<sup>7)</sup> classifies the sinter to three different types based on the short basicity ( $B2 = Y_{\text{CaO}}/Y_{\text{SiO}_2}$ ): acid ( $B2 < 1.0$ ), fluxed ( $1.0 < B2 < 2.5$ ) and super-fluxed ( $B2 > 2.5$ ) sinter, of which the most common type is the fluxed sinter.  $Y_i$  in the formula refers to the mass fraction of the component  $i$ .

Mochón *et al.*<sup>13)</sup> point out that it is important to have a sinter with a high iron content, a low gangue content and short basicity of 1.6–2.1. Wang *et al.*<sup>14)</sup> continue that a high-quality sinter should have characteristics of high strength, low reduction degradation and easy reduction. These metallurgical properties are closely related to the structural characteristics of the sinter. For example, the pore size and distribution of the sinter greatly influence the strength and reduction.<sup>14)</sup>

### 2.1. Chemical Composition

Chemical compositions of sinters may be presented in various ways depending on the methods that have been used in chemical analysis. The main characterisation method for chemical composition is X-ray fluorescence (XRF). As mentioned above, iron is the element with the largest quantity in all sinters and despite its existence in sinters as oxides its amount is usually presented as “Total Fe ( $\text{Fe}_{\text{tot}}$ )”, which refers to elemental composition as mass%. To illustrate the distinction between divalent and trivalent iron, the amount of divalent iron (as FeO) is usually shown separately. It should be noted that this should not be confused with the mineralogical composition, and divalent oxide is most

likely to appear as a part of other minerals than wüstite. Furthermore, the amounts of the most other components are expressed as contents of corresponding oxides, although there are some exceptions such as sulphur.

Typical compositions of iron ore sinters are shown in **Table 1** after Pettersson *et al.*,<sup>15)</sup> Fernández-González *et al.*<sup>3)</sup> and Cores *et al.*,<sup>16)</sup> whereas **Table 2** collects examples of sinter compositions (both production and laboratory sinters) from various sources.<sup>10,12,15–21)</sup> Table 2 shows that sinters from different production sites are chemically quite similar. However, Heinänen<sup>10)</sup> emphasizes that some seemingly insignificant differences in the chemical composition are in fact significant in regard to sinter properties, for example the contents of Fe, MgO and  $\text{Al}_2\text{O}_3$  as well as basicity.

Because world’s reserve of high-grade iron ores is declining, the gangue minerals of iron ore, such as  $\text{SiO}_2$  and  $\text{Al}_2\text{O}_3$ , have been increasing.<sup>22,23)</sup> Ores with higher gangue contents do not allow to produce sinters with lower  $\text{SiO}_2$  contents and correspondingly higher Fe contents.<sup>24)</sup> In general, as the  $\text{Al}_2\text{O}_3$  content of iron ores increases, both the sintering performance and the quality of the sinter product deteriorate.<sup>22)</sup> For example, the  $\text{SiO}_2$  content in the sinter of Thyssenkrupp Steel Europe AG has risen from values of under 5.4 mass% to 5.9 mass% during the years 2000–2015, along with a decrease of the Fe contents in sinter from 57.5 mass% to 55 mass%.<sup>25)</sup> Quite similarly, the contents of  $\text{SiO}_2$  and  $\text{Al}_2\text{O}_3$  ranged from 5.2 mass% to 7.7 mass% and from 1.0 mass% to 2.4 mass% in a 3-year period from 2012 to 2015 at Redcar blast furnace owned by SSI UK.<sup>26)</sup> To counter the adverse impact of alumina on sinter quality, MgO fluxes are often used to improve the high-temperature properties of sinters.<sup>23)</sup>

The chemical compositions of iron ore sinters collected in Tables 1 and 2 show that the major components in the sinter system are FeO,  $\text{Fe}_2\text{O}_3$ , CaO,  $\text{SiO}_2$ , MgO and  $\text{Al}_2\text{O}_3$ . With this kind of a six-component system, approximately 99% of the system can be described.

### 2.2. Mineralogical Composition

In principle, the chemical components of the sinter presented in chapter 2.1 form a large variety of mineral compounds. Thus, the mineralogy of iron ore sinters is quite complex.<sup>27)</sup> The characterisation of the phases in sinter is usually performed manually by an experienced mineralogist (point counting) using a microscope.<sup>28)</sup> With the advancement of science and technology, there are an increased number of methods to characterise the composition and structure of mineral phases in sinter. The current main characterization methods are optical microscopy (OM), scanning electron microscopy (SEM) equipped with energy dispersive spectroscopy (EDS), X-ray diffraction (XRD), transmission

**Table 1.** Typical chemical compositions of ironmaking sinters (in mass%).

Site	Value type	$\text{Fe}_{\text{tot}}$	FeO	$\text{SiO}_2$	MgO	$\text{Al}_2\text{O}_3$	Alkalis	P	B2
European countries <sup>15)</sup>	Typical	~56.5	7.3±0.5	5.9±0.2	1.0±0.2				2.0±0.1
Western European countries <sup>3)</sup>	Typical	>56			1.65	1.35			1.7
Western European countries <sup>16)</sup>	Minimum	51	4.0	5.3	0.7	0.6			
Western European countries <sup>16)</sup>	Maximum	61	11	5.4	2.2	1.8	0.11	0.04	

**Table 2.** Examples of chemical compositions of iron ore sinters (in mass%).

Reference	Major components								Minor components					Basicity		
	Fe <sub>tot</sub>	FeO	Fe <sub>2</sub> O <sub>3</sub> ***	CaO	SiO <sub>2</sub>	MgO	Al <sub>2</sub> O <sub>3</sub>	Sum	MnO	TiO <sub>2</sub>	S	P	V	Na <sub>2</sub> O	K <sub>2</sub> O	B2
<b>Production sinters</b>																
Iljana <i>et al.</i> <sup>17)</sup>	60.6	11.1	74.3	7.12	3.35	1.99	0.58	98.5						0.050	2.13	
Honeyands <i>et al.</i> <sup>18)</sup>	57.38	5.45	76.0	9.24	5.56	0.95	1.80	99.0			0.06				1.66	
Honeyands <i>et al.</i> <sup>18)</sup>	56.73	5.91	74.5	10.04	5.43	1.76	1.87	99.6			0.07				1.85	
Heinänen <sup>10)</sup>	59.9	10.9	73.5	7.13	4.63	2.20	0.76	99.2							1.54	
Heinänen <sup>10)</sup>	59.6	11.5	72.4	7.07	5.47	1.72	0.84	99.0							1.29	
Heinänen <sup>10)</sup>	60.0	11.1	73.5	6.76	5.51	1.50	0.75	99.1							1.23	
Heinänen <sup>10)</sup>	57.0	5.6	75.3	10.18	5.86	1.95	1.10	100.0							1.74	
Heinänen <sup>10)</sup>	57.1	6.1	74.9	9.62	5.71	1.79	1.51	99.6							1.69	
Heinänen <sup>10)</sup>	56.8	6.3	74.2	9.62	5.76	1.92	1.23	99.0							1.67	
Heinänen <sup>10)</sup>	58.0	4.9	77.5	8.80	5.66	1.66	1.05	99.6							1.55	
<i>Average</i>								99.2								
<b>Laboratory sinters</b>																
Higuchi <i>et al.</i> <sup>12)</sup>	62.7	9.60	79.0	5.20	3.61	1.13	0.96	99.5							1.44	
Higuchi <i>et al.</i> <sup>12)</sup>	57.7	4.51	77.5	9.02	4.93	0.97	1.72	98.6							1.83	
Honeyands <i>et al.</i> <sup>18)</sup>	56.87	4.45	76.4	9.83	4.95	1.79	1.73	99.1			0.05				1.99	
Pownceby <i>et al.</i> <sup>19)</sup>			77.1	14.16	3.48	0.12	4.56	99.4	0.15		0.02**		0.10		4.07	
Umadevi <i>et al.</i> <sup>20)</sup>	54.8	9.3	68.0	12.0	5.94	1.48	3.60	100.3					0.050	0.090	2.02	
Umadevi <i>et al.</i> <sup>20)</sup>	54.0	9.6	66.5	12.6	6.20	1.85	3.65	100.4					0.530	0.080	2.03	
Umadevi <i>et al.</i> <sup>20)</sup>	53.7	9.8	65.9	13.0	6.30	2.18	3.72	100.9					0.547	0.090	2.06	
Umadevi <i>et al.</i> <sup>20)</sup>	53.2	10.2	64.7	13.6	6.60	2.54	3.83	101.5					0.523	0.876	2.06	
Yan <i>et al.</i> <sup>21)</sup>	57.87	8.98	72.8	9.82	4.79	1.57	1.89	99.8						0.111*	2.05	
Pettersson <i>et al.</i> <sup>15)</sup>	56.06	7.08	72.3	11.7	5.92	1.04	1.14	99.2	0.47*	0.07		0.028	0.004		1.98	
Pettersson <i>et al.</i> <sup>15)</sup>	56.32	7.21	72.5	11.7	5.88	1.03	0.96	99.3	0.39*	0.124		0.027	0.003		1.99	
Pettersson <i>et al.</i> <sup>15)</sup>	56.16	7.81	71.6	11.8	5.88	0.99	1.07	99.2	0.37*	0.108		0.045	0.015		2.01	
Pettersson <i>et al.</i> <sup>15)</sup>	56.02	7.17	72.1	11.9	5.96	1.07	1.02	99.3	0.39*	0.096		0.026	0.02		2.00	
Cores <i>et al.</i> <sup>16)</sup>	57.5	5.5	76.1	9.15	5.7	1.55	1.16	99.2	0.64		0.012	0.034		0.041	0.066	1.62
Cores <i>et al.</i> <sup>16)</sup>	56.3	5.7	74.2	10.45	5.6	1.71	1.35	99.0	0.72		0.013	0.041		0.038	0.060	1.87
Cores <i>et al.</i> <sup>16)</sup>	57.1	3.5	77.8	9.25	5.6	1.63	1.17	98.9	0.66		0.010	0.030		0.039	0.064	1.59
Cores <i>et al.</i> <sup>16)</sup>	56.0	3.2	76.5	11.10	5.4	1.53	1.15	98.9	0.64		0.017	0.031		0.038	0.065	2.02
Cores <i>et al.</i> <sup>16)</sup>	57.1	5.0	76.1	9.20	5.8	1.44	1.24	98.8	0.65		0.012	0.041		0.038	0.058	1.59
Cores <i>et al.</i> <sup>16)</sup>	56.2	4.6	75.2	10.90	5.7	1.58	1.15	99.2	0.68		0.015	0.039		0.039	0.058	1.93
Cores <i>et al.</i> <sup>16)</sup>	57.5	3.3	78.5	9.10	5.4	1.51	1.20	99.1	0.66		0.011	0.038		0.037	0.060	1.70
Cores <i>et al.</i> <sup>16)</sup>	56.7	4.3	76.3	10.40	5.5	1.50	1.17	99.2	0.70		0.018	0.040		0.037	0.056	1.90
Cores <i>et al.</i> <sup>16)</sup>	57.3	5.7	75.6	9.35	5.4	1.70	1.22	99.0	0.74		0.011	0.042		0.039	0.071	1.73
Cores <i>et al.</i> <sup>16)</sup>	56.6	5.6	74.7	10.50	5.3	1.68	1.17	99.0	0.72		0.014	0.039		0.037	0.071	1.98
Cores <i>et al.</i> <sup>16)</sup>	57.6	3.7	78.2	8.80	5.4	1.60	1.19	98.9	0.80		0.013	0.040		0.036	0.072	1.64
Cores <i>et al.</i> <sup>16)</sup>	56.9	3.6	77.4	10.35	4.9	1.61	1.16	99.0	0.71		0.018	0.040		0.031	0.068	2.13
Cores <i>et al.</i> <sup>16)</sup>	58.0	4.7	77.7	8.60	5.2	1.62	1.20	99.0	0.75		0.012	0.040		0.032	0.066	1.67
Cores <i>et al.</i> <sup>16)</sup>	56.5	5.0	75.2	10.13	5.7	1.66	1.10	98.8	0.73		0.014	0.036		0.036	0.072	1.82
Cores <i>et al.</i> <sup>16)</sup>	56.7	3.5	77.2	9.05	5.0	1.56	1.19	97.5	0.79		0.012	0.041		0.040	0.075	1.81
Cores <i>et al.</i> <sup>16)</sup>	57.0	4.5	76.5	9.90	5.5	1.49	1.17	99.1	0.77		0.015	0.039		0.039	0.076	1.80
Cores <i>et al.</i> <sup>16)</sup>	57.0	5.7	75.2	10.35	5.9	1.75	1.02	99.9	1.04		0.013	0.036		0.036	0.065	1.75
Cores <i>et al.</i> <sup>16)</sup>	55.5	5.2	73.6	10.85	5.5	1.65	0.99	97.8	0.96		0.022	0.030		0.042	0.070	1.97
Cores <i>et al.</i> <sup>16)</sup>	56.2	5.5	74.2	10.85	5.7	1.55	0.91	98.8	0.94		0.017	0.031		0.038	0.064	1.90
Cores <i>et al.</i> <sup>16)</sup>	56.0	3.8	75.8	10.80	5.6	1.65	1.06	98.8	0.93		0.023	0.035		0.045	0.078	1.93
Cores <i>et al.</i> <sup>16)</sup>	55.4	3.9	74.9	11.10	5.8	1.68	1.11	98.5	0.99		0.020	0.029		0.042	0.078	1.91
Cores <i>et al.</i> <sup>16)</sup>	54.9	3.5	74.6	11.55	6.0	1.68	1.15	98.5	0.93		0.025	0.032		0.041	0.079	1.94
Cores <i>et al.</i> <sup>16)</sup>	55.7	5.5	73.5	11.55	5.6	1.88	1.12	99.2	0.85		0.015	0.035		0.041	0.092	2.01
Cores <i>et al.</i> <sup>16)</sup>	56.1	5.3	74.3	10.10	5.3	1.70	1.18	97.9	0.80		0.012	0.034		0.039	0.091	1.91
Cores <i>et al.</i> <sup>16)</sup>	56.5	5.2	75.0	10.10	5.2	1.69	1.22	98.4	0.97		0.014	0.032		0.042	0.088	1.94
Cores <i>et al.</i> <sup>16)</sup>	55.3	4.4	74.2	11.00	5.7	2.01	1.27	98.6	0.80		0.015	0.037		0.044	0.095	1.95
<i>Average</i>								99.1								

\* Reported as elemental compound in the original publication but converted here to oxide compound.

\*\* Reported as oxide compound in the original publication but converted here to elemental compound.

\*\*\* Calculated here taking into account the contents of Fe<sub>tot</sub> and FeO reported in the original publication.

electron microscopy (TEM), and serial sectioning and 3D reconstruction.<sup>14)</sup> The SEM can be automated and equipped with a motorized and computer-controlled multiple sample stage as introduced by Wang *et al.*<sup>29)</sup> In addition to manual methods, micro image processing software packages, such as VisuMet developed by K1-Met, are used nowadays to identify the main mineral phases in sinter.<sup>30)</sup>

Sinters are primarily composed of iron oxides<sup>19,31)</sup> (hematite, Fe<sub>2</sub>O<sub>3</sub> and magnetite, Fe<sub>3</sub>O<sub>4</sub>), complex calcium ferrite phases<sup>19,31)</sup> (mainly silico-ferrite of calcium and aluminium, SFCA), crystalline calcium-rich silicates,<sup>19)</sup> residual slag<sup>31)</sup> solidified as amorphous phases, and non-assimilated non-ferrous particles,<sup>19)</sup> which are not reacted during sintering. Among them, hematite and SFCA are in main proportion.<sup>31)</sup> Iron oxides exist either in an unreacted primary form or as secondary phases formed by reactions or precipitation from the melt.<sup>27,31)</sup> Hsieh and Whiteman<sup>32–34)</sup> have found that the gas atmosphere used in sintering and the compositions of raw materials have significant effects on the mineral phases that are formed.

Different phases verified in the sinter have been collected from literature to **Table 3**, in which the sinter phases have been classified into iron oxides, calcium ferrites, amorphous silicates, crystalline silicates and non-assimilated non-ferrous particles. The classification has been modified after Mezibricky *et al.*<sup>35)</sup> In addition to mineral phases, there are different-sized pores<sup>8,12,27,28,36–38)</sup> in the sinter structure, which also have a marked effect on the sinter properties.<sup>14)</sup>

As earlier stated, the chemical composition together with the process conditions determine the mineral compounds in the sinter. According to Hsieh and Whiteman,<sup>34)</sup> an increase in short basicity favours the formation of calcium ferrite. The amount of calcium ferrite or SFCA phases is also increased with the increase of Al<sub>2</sub>O<sub>3</sub> content, and simultaneously the amounts of amorphous silicates and reoxidised hematite decrease. Use of dolomite increases the MgO content, which leads to a decrease in the amount of calcium ferrites. Otherwise, if the increase in the amount of MgO is due to serpentine addition, the content of calcium ferrite increases considerably.<sup>34)</sup>

### 2.2.1. Iron Oxides

Hematite, Fe<sub>2</sub>O<sub>3</sub>, is a dominant mineral in sinter and is always present in varying proportions. The hematite in sinter can be classified into: primary hematite, which is relict hematite from the iron ore concentrate; and secondary hematite, which is crystallized from the melt.<sup>10)</sup> If coarse and dense hematite exists in the iron ore, some unreacted primary hematite may exist in the sinter.<sup>34)</sup>

Magnetite, Fe<sub>3</sub>O<sub>4</sub>, is a dominant mineral in sinter and similarly to hematite the amount of magnetite depends largely on the magnetite/hematite ratio in the sinter mix. Sinter contains several different types of magnetite and they can be classified into: primary magnetite, which is relict magnetite originating from the iron ore concentrate; secondary magnetite, which is magnetite crystallized from the melt; and magnetite reduced from hematite.<sup>10)</sup>

Wüstite is relatively rare in industrial sinters and only small amounts of it can be found in acid sinters.<sup>10)</sup>

**Table 3.** Sinter phases reported in the literature.

Phase	Formula	Reference
<b>Iron oxides</b>		
Hematite	Fe <sub>2</sub> O <sub>3</sub>	12,18,27,30,34–40)
Primary hematite (non-assimilated or residual)		8,16,18,28,41)
Secondary hematite (precipitated)		8,16,18,28,41)
Magnetite	Fe <sub>3</sub> O <sub>4</sub>	12,18,27,28,30,34–42)
Primary magnetite (non-assimilated or residual)		16)
Secondary magnetite (precipitated)		16)
Wüstite	Fe <sub>1–y</sub> O	27,35,39)
<b>Calcium ferrites</b>		
SFCA		8,12,16,18,27,28,36,38,40,42)
SFCA-I		18,27,28,42)
Calcium ferrites	<i>e.g.</i> Ca <sub>4</sub> Fe <sub>9</sub> O <sub>17</sub> , CaFe <sub>5</sub> O <sub>7</sub> , Ca <sub>2</sub> Fe <sub>22</sub> O <sub>33</sub>	30,34,35,37,38,40,41)
Monocalcium ferrite, CF	CaFe <sub>2</sub> O <sub>4</sub>	27)
Dicalcium ferrite, C2F	Ca <sub>2</sub> Fe <sub>2</sub> O <sub>5</sub>	27)
Brownmillerite	Ca <sub>2</sub> (Al,Fe) <sub>2</sub> O <sub>5</sub>	35)
Calcium iron oxides		39)
<b>Amorphous silicates</b>		
Slag		37)
Glass		18,19,27,28,30,42)
Glassy silicate/siliceous glass		30,34,41)
Silicate		38)
<b>Crystalline silicates</b>		
Fayalite	Fe <sub>2</sub> SiO <sub>4</sub>	37)
Calcium silicate		37)
Dicalciumsilicate/larnite, C2S	Ca <sub>2</sub> SiO <sub>4</sub>	18,27,35,39)
Fe–Ca-olivine	(Ca,Fe,Mg) <sub>2</sub> (Si,Al)O <sub>4</sub>	27)
Kirschsteinite	CaFeSiO <sub>4</sub>	27)
Hedenbergite	CaFeSi <sub>2</sub> O <sub>6</sub>	27,35)
(Pseudo)wollastonite	CaSiO <sub>3</sub>	27,35)
<b>Non-assimilated non-ferrous particles</b>		
(Relict) flux		8,34)
Quartz	SiO <sub>2</sub>	18,27,35,39)
Calcite	CaCO <sub>3</sub>	39)
Dolomite	MgCa(CO <sub>3</sub> ) <sub>2</sub>	35,39)
Lime	CaO	35,39)
Gangue		16)

### 2.2.2. Calcium Ferrites and SFCAs

According to several authors, no pure calcium ferrites are present in sinter as calcium ferrites contain so much dissolved silicon and aluminium that they can be called SFCA (silico-ferrite of calcium and aluminium) phases. Those phases are key bonding minerals within industrial iron ore

sinter.<sup>43,44</sup> Needle-like structures of calcium ferrites have a relatively open structure and are easily accessible for reduction gas in the blast furnace.<sup>7)</sup>

Several authors reported on the existence and the importance of calcium ferrites as mineral phases in sinter already in the late 1950s and early 1960s.<sup>40)</sup> However, due to limited observation techniques and analytical methods of that time, calcium ferrites were considered as belonging to relatively simple systems of CaO–Fe<sub>2</sub>O<sub>3</sub> and CaO–FeO–Fe<sub>2</sub>O<sub>3</sub>.<sup>40)</sup> A revolution occurred at the beginning of the 1960s, when Hancart<sup>45)</sup> discovered ‘impure ferrites’ when exposing iron ore sinters to X-ray diffraction. A couple of years later, with the use of electron probe microanalysis (EPMA), Hancart *et al.*<sup>46)</sup> determined the chemical composition of those complex ferrites. Those authors proposed a general formula for the calcium ferrites existing in iron ore sinters  $x\text{Fe}_2\text{O}_3 \cdot y\text{SiO}_2 \cdot z\text{Al}_2\text{O}_3 \cdot 5\text{CaO}$  with  $x + y + z = 12$ .<sup>40,47)</sup> The abbreviation SFCA was then created to denote the calcium ferrites found in iron ore sinter.<sup>40)</sup>

The SFCA in iron ore sinter has been categorized in the literature on the basis of composition, morphology and crystal structure into two main types.<sup>44)</sup> The first is a high-Fe, low-Si form called SFCA-I, which has a characteristic platy (also described as acicular) morphology.<sup>44)</sup> Mumme *et al.*<sup>48)</sup> reported that an SFCA-I phase in an industrial sinter contained 84 mass% Fe<sub>2</sub>O<sub>3</sub>, 13 mass% CaO, 1 mass% SiO<sub>2</sub> and 2 mass% Al<sub>2</sub>O<sub>3</sub>, and also a synthesized SFCA-I material with the composition 83.2 mass% Fe<sub>2</sub>O<sub>3</sub>, 12.6 mass% CaO and 4.2 mass% Al<sub>2</sub>O<sub>3</sub>. The second SFCA type is a low-Fe form called SFCA, which is described as having a prismatic or columnar morphology.<sup>44)</sup> The SFCA phase found in industrial sinters typically contains 60–76 mass% Fe<sub>2</sub>O<sub>3</sub>, 13–16 mass% CaO, 3–10 mass% SiO<sub>2</sub>, 4–10 mass% Al<sub>2</sub>O<sub>3</sub> and 0.7–1.5 mass% MgO.<sup>44)</sup> The SFCA and SFCA-I phases are formed in iron ore sintering operations.<sup>49)</sup> Additionally, Mumme<sup>50)</sup> has described a third SFCA homologue, denoted SFCA-II (A<sub>4</sub>T<sub>14</sub>M<sub>16</sub>O<sub>48</sub>), synthesized in the ternary CaO–Fe<sub>2</sub>O<sub>3</sub>–Al<sub>2</sub>O<sub>3</sub> system. It is not known if SFCA-II is formed in industrial sinter.<sup>42)</sup> These SFCA (A<sub>2</sub>T<sub>6</sub>M<sub>6</sub>O<sub>20</sub>), SFCA-I (A<sub>3</sub>B<sub>8</sub>T<sub>8</sub>O<sub>28</sub>) and SFCA-II (A<sub>4</sub>T<sub>14</sub>M<sub>16</sub>O<sub>48</sub>) phases are homologous series based on that of aenigmatite.<sup>48,50,51)</sup> In the structure formula, A = Ca<sup>2+</sup>, B = Ca<sup>2+</sup> and Fe<sup>2+</sup>, and M and T indicate the octahedral and the tetrahedral cation sites, respectively.<sup>11)</sup>

### 2.2.3. Amorphous and Crystalline Silicates

Silicates in the sinter can either be in the crystalline or amorphous form. Crystalline silicates (*e.g.* hedenbergite, kirschsteinite, dicalciumsilicate) are formed in the sintering process and are usually rich in calcium.<sup>10,19)</sup> Amorphous silicates do not have crystal structure and those have solidified from residual slag. The amorphous silicates are primarily composed of CaO, FeO, Fe<sub>2</sub>O<sub>3</sub> and SiO<sub>2</sub>.<sup>10)</sup> If the iron oxides exists either in the divalent or trivalent form, depends on the formation conditions such as temperature, composition and oxygen partial pressure.

### 2.2.4. Non-assimilated Non-ferrous Particles

Non-assimilated non-ferrous particles are minerals (*e.g.* quartz, olivine, lime) in the raw material mix, which have not reacted during sintering. In addition to non-ferrous

phases, iron oxides (hematite and magnetite) can partly stay unreacted during sintering.<sup>10)</sup>

## 3. Phase Equilibria in Sinter Systems

Based on the chemical and mineralogical compositions presented in chapter 2, it can be concluded which components should be considered when studying sinter systems with phase diagrams. A compilation of the systems of interest is presented in **Table 4**. In order to study the complete sinter system taking into account all major components, a six-component system with FeO, Fe<sub>2</sub>O<sub>3</sub>, CaO, SiO<sub>2</sub>, MgO and Al<sub>2</sub>O<sub>3</sub> should be considered.

In addition to the sinter and its behaviour in ironmaking processes such as the blast furnace, the understanding of the FeO–Fe<sub>2</sub>O<sub>3</sub>–CaO–SiO<sub>2</sub>–MgO–Al<sub>2</sub>O<sub>3</sub> system is crucially important in various metallurgical and other industrial applications (such as studying cements, slags, ash, inclusions, glasses or refractory materials).<sup>52–55)</sup> Hence, it is not surprising that the phase equilibria of these systems have been studied comprehensively. In order to collect a more comprehensive review on the studies of the above mentioned FeO–Fe<sub>2</sub>O<sub>3</sub>–CaO–SiO<sub>2</sub>–MgO–Al<sub>2</sub>O<sub>3</sub> system, some studies which have originally focused on other topics than sintering, have also been included in this study due to the fact that their results are applicable for studying the sinter system, too.

Phase equilibria of different systems can be studied either experimentally or computationally. Experimental studies (with either equilibrium or dynamic measurements) are required when starting to study new systems with components whose thermodynamic behaviour is not known. Experimental measurement of the phase equilibria and construction of phase diagrams (especially with equilibrium method) is time-consuming, expensive and requires extreme accuracy. Furthermore, the addition of new components in the already studied systems requires a new set of experiments. Therefore, computational methods in the construction of phase diagrams are more common as long as sufficient amount of thermochemical data with sufficient accuracy is available from the previous experimental studies. Nowadays, it is possible to construct innumerable amount of phase diagrams of multicomponent oxide systems using thermochemical software and their databases. These software enable the construction of subsystem sections of the multicomponent systems, for which the complete phase diagram would be impossible to visualise. The most essential – and basically the only – requirement for this computational approach is the availability of accurate ther-

**Table 4.** The most significant components in the sinter system.

Studied system	Main components of interest	Additional components of interest
Iron oxides	FeO, Fe <sub>2</sub> O <sub>3</sub>	
Calcium ferrites	CaO, Fe <sub>2</sub> O <sub>3</sub>	FeO
SFCA	FeO, Fe <sub>2</sub> O <sub>3</sub> , SiO <sub>2</sub> , CaO, Al <sub>2</sub> O <sub>3</sub>	
Silicates	SiO <sub>2</sub> , CaO, FeO	Al <sub>2</sub> O <sub>3</sub> , MgO
Complete sinter system	FeO, Fe <sub>2</sub> O <sub>3</sub> , CaO, SiO <sub>2</sub> , MgO, Al <sub>2</sub> O <sub>3</sub>	TiO <sub>2</sub> , MnO, Na <sub>2</sub> O

mochemical data for the system of interest.

A CALPHAD method (originally “Calculation of phase diagrams”; later expanded to refer to “Computer coupling of phase diagrams and thermochemistry”) in which thermochemical data (*i.e.* suitable mathematical expressions to model the non-ideality of solution phases as well as values of the parameters included in these models) is optimized based on all available experimental data and then used to simulate computationally the experimentally constructed phase diagrams is nowadays widely used in many applications. One of its strengths is the ability to predict the behaviour of more complex systems with the extrapolation of the data of lower order subsystems.<sup>52,56,57)</sup>

The experimental determination of phase equilibria and phase diagrams is still important when studying systems with new sets of components, when studying known systems in new conditions or when adjusting existing models with more detailed or accurate data. However, it is nowadays more convenient and common to construct the phase diagrams for each individual case computationally rather than collect and use vast libraries of existing phase diagrams, each of which was determined experimentally. A comprehensive collection of experimentally determined phase diagrams of lower order subsystems of the FeO–Fe<sub>2</sub>O<sub>3</sub>–CaO–SiO<sub>2</sub>–MgO–Al<sub>2</sub>O<sub>3</sub> system (among various other oxide systems) was published in 1995 by VDEh. This “Slag Atlas” collects the results of the studies that had been published until mid-1990s.<sup>58)</sup> **Table 5** lists all the phase diagrams available in the “Slag Atlas” for the subsystems of the sinter system together with the references to the experimental phase diagram studies of these systems subsequent to 1995. It should be noted that the “Slag Atlas” is a review compilation in itself and references to original studies are not repeated here since they can be found in the “Slag Atlas”.

In addition to existing diagrams mentioned in Table 5, designated sections of the multicomponent systems – as well as phase diagrams of more simple subsystems – can be constructed from assessed thermochemical data using thermochemical software and their databases. A list of studies, in which assessment and optimization of thermochemical data has been done with the CALPHAD method for the systems containing FeO, Fe<sub>2</sub>O<sub>3</sub>, CaO, SiO<sub>2</sub>, MgO and/or Al<sub>2</sub>O<sub>3</sub>, is collected to **Table 6**. In Table 6 it is also mentioned, which solution models have been used in different studies to describe the non-ideality of molten and solid solution phases such as monoxide, olivine, spinel, pyroxene, mullite and melilite.

As seen from Table 6, thermodynamic data has been collected and assessed for the systems containing all six components needed to study the phase equilibria in sinters. This thermochemical data is available in the databases of thermochemical software such as FactSage,<sup>129–131)</sup> ThermoCalc,<sup>119)</sup> MTDATA,<sup>54,132)</sup> CEQCSI<sup>133)</sup> and MPE,<sup>127,128)</sup> all of which can be used to construct required sections of the FeO–Fe<sub>2</sub>O<sub>3</sub>–SiO<sub>2</sub>–CaO–MgO–Al<sub>2</sub>O<sub>3</sub> system. However, it should be noted that although all the components of the FeO–Fe<sub>2</sub>O<sub>3</sub>–SiO<sub>2</sub>–CaO–MgO–Al<sub>2</sub>O<sub>3</sub> system are taken into account in all the software mentioned in Table 6, data concerning some of the relevant phases may not be included in all the databases of these software.<sup>54,55,121–123,132,134)</sup> Based on the information provided in the references of Table 6 as well as in the documentation on the software websites, **Table 7**, which

collects the possibilities to model the solution phases potentially existing in iron ore sinters with different software, has been compiled. The vast number of stoichiometric phases included in the databases are not mentioned in the table. Empty spaces in Table 7 indicate that either the particulate phase cannot be modelled with the software in question, or the documentation of the databases lacks the information concerning this phase. Based on the Table 7, it can be seen that the major needs for the further research are in the accurate and reliable modelling of the SFCA phases. It should also be noted that the addition of accurate thermochemical data of SFCA phases to the existing databases also requires more detailed understanding on the composition, crystallography, morphology and formation of SFCA phases as classified in more detail by Nicol *et al.*<sup>135)</sup> in their review.

It is also seen from Tables 6 and 7 that different approaches have been used to model the non-ideality of solution phases in different software. For example, the molten oxide phase is described with the modified quasichemical model (MQM)<sup>56,87,136–139)</sup> in FactSage’s (GTT) FToxid database,<sup>129–131,134)</sup> with the associate model (AM)<sup>56,91,120)</sup> in MTDATA’s (NPL) NPLOX database,<sup>54,132,134)</sup> with the cell model (CM)<sup>56,140,141)</sup> in CEQCSI’s (IRSID)<sup>123,125,126,133,134)</sup> and MPE’s (CSIRO)<sup>127,128,134)</sup> oxide databases and with either cell model<sup>56,140,141)</sup> or associate model<sup>56,91,120)</sup> in ThermoCalc’s SLAG2 and NOX3 databases, respectively.<sup>134)</sup> Furthermore, the generalized central atom model (GCA)<sup>124,126)</sup> developed based on the cell model has also been used to model both oxide and metal phases in CEQCSI,<sup>125)</sup> whereas the reciprocal ionic liquid model (RILM),<sup>56,142)</sup> which assumes two sublattices in liquid oxide phase has been used in ThermoCalc’s own ION3 -oxide database.<sup>119,134)</sup> For solid solutions more uniform approach is used, since the sublattice model based on compound energy formalism (CEF)<sup>56,143–145)</sup> is used in most cases.<sup>132,134)</sup> An excellent and more detailed overview on thermodynamic models and their application in different areas of metallurgy has been made by Jung.<sup>134)</sup>

In addition to the systems collected to Table 6, thermodynamic data has also been assessed for the systems containing minor components (such as sodium, titanium, manganese, phosphorus and boron) of the sinter systems: *e.g.* Na<sub>2</sub>O–FeO–Fe<sub>2</sub>O<sub>3</sub>–Al<sub>2</sub>O<sub>3</sub>–SiO<sub>2</sub> system by Moosavi-Khoonsari *et al.*,<sup>146)</sup> TiO<sub>2</sub>–Ti<sub>2</sub>O<sub>3</sub>–FeO–Fe<sub>2</sub>O<sub>3</sub>–Al<sub>2</sub>O<sub>3</sub>–MgO system by Jantzen *et al.*,<sup>147)</sup> MnO–FeO<sub>x</sub>–MO<sub>x</sub> (MO<sub>x</sub> = PO<sub>2.5</sub>, SiO<sub>2</sub>, AlO<sub>1.5</sub>, MgO, CaO) system by Suito *et al.*,<sup>148)</sup> MnO–FeO–CaO–SiO<sub>2</sub>–MgO–Al<sub>2</sub>O<sub>3</sub> system by Duan *et al.*,<sup>149)</sup> MnO–CaO–MgO–SiO<sub>2</sub>–Al<sub>2</sub>O<sub>3</sub> system by Zhao *et al.*,<sup>150)</sup> MnO–P<sub>2</sub>O<sub>5</sub>–FeO<sub>x</sub>–CaO–SiO<sub>2</sub>–Al<sub>2</sub>O<sub>3</sub> system by Zhu *et al.*<sup>151)</sup> as well as binary and ternary systems containing B<sub>2</sub>O<sub>3</sub> (with MgO, CaO and SiO<sub>2</sub>) by Sunkar *et al.*<sup>152)</sup>

#### 4. Discussion on Practical Relevance

Phase diagrams as well as computations with thermodynamic data (presented in chapter 3) provide useful tools to study the behaviour of sinters in varying conditions (*i.e.* temperature and atmosphere). This chapter illustrates the use of these thermodynamic tools in sinter related research and development using studies about phase stabilities of the FeO<sub>x</sub>–SiO<sub>2</sub>–CaO(–Al<sub>2</sub>O<sub>3</sub>) system in sintering conditions as examples. This system has been chosen as an example due

**Table 5.** Phase diagrams available for the subsystems of the FeO–Fe<sub>2</sub>O<sub>3</sub>–CaO–SiO<sub>2</sub>–MgO–Al<sub>2</sub>O<sub>3</sub> system (based on Slag Atlas<sup>58</sup>) with additions from more recent sources).

Components						Type of diagram	Reference
FeO	Fe <sub>2</sub> O <sub>3</sub>	CaO	SiO <sub>2</sub>	MgO	Al <sub>2</sub> O <sub>3</sub>		
<b>Binary subsystems</b>							
X	X					Binaries: Fe–O; FeO–Fe <sub>2</sub> O <sub>3</sub> . T–p(O <sub>2</sub> ) for Fe–O system.	Slag Atlas <sup>58</sup> *
X		X				<i>cf.</i> ternary FeO–Fe <sub>2</sub> O <sub>3</sub> –CaO system.**	Slag Atlas <sup>58</sup> *
X			X			<i>cf.</i> ternary FeO–Fe <sub>2</sub> O <sub>3</sub> –SiO <sub>2</sub> system.**	Slag Atlas <sup>58</sup> *
X				X		<i>cf.</i> ternary FeO–Fe <sub>2</sub> O <sub>3</sub> –MgO system.**	Slag Atlas <sup>58</sup> *
X					X	<i>cf.</i> ternary FeO–Fe <sub>2</sub> O <sub>3</sub> –Al <sub>2</sub> O <sub>3</sub> system.**	Slag Atlas <sup>58</sup> *
	X	X				<i>cf.</i> ternary FeO–Fe <sub>2</sub> O <sub>3</sub> –CaO system.**	Slag Atlas <sup>58</sup> *
	X		X			<i>cf.</i> ternary FeO–Fe <sub>2</sub> O <sub>3</sub> –SiO <sub>2</sub> system.**	Slag Atlas <sup>58</sup> *
	X			X		<i>cf.</i> ternary FeO–Fe <sub>2</sub> O <sub>3</sub> –MgO system.**	Slag Atlas <sup>58</sup> *
	X				X	<i>cf.</i> ternary FeO–Fe <sub>2</sub> O <sub>3</sub> –Al <sub>2</sub> O <sub>3</sub> system.**	Slag Atlas <sup>58</sup> *
		X	X			Binary: CaO–SiO <sub>2</sub> .	Slag Atlas <sup>58</sup> *
		X		X		Binary: CaO–MgO.	Slag Atlas <sup>58</sup> *
		X			X	Binary: CaO–Al <sub>2</sub> O <sub>3</sub> .	Slag Atlas <sup>58</sup> *
			X	X		Binary: MgO–SiO <sub>2</sub> .	Slag Atlas <sup>58</sup> *
			X		X	Binary: Al <sub>2</sub> O <sub>3</sub> –SiO <sub>2</sub> .	Slag Atlas <sup>58</sup> *
				X	X	Binary: MgO–Al <sub>2</sub> O <sub>3</sub> .	Slag Atlas <sup>58</sup> *
<b>Ternary subsystems</b>							
X	X	X				Pseudobinaries: FeO <sub>x</sub> –CaO (in eq. with met. Fe; in air; in pure oxygen).	Slag Atlas <sup>58</sup> *
X	X	X				Ternaries: Liquidus projection for FeO–Fe <sub>2</sub> O <sub>3</sub> –CaO system. /Iso-T sections for FeO–Fe <sub>2</sub> O <sub>3</sub> –CaO system in 1 450°C, 1 500°C and 1 550°C.	Slag Atlas <sup>58</sup> *
X	X	X				Iso-T sections for Fe–Fe <sub>2</sub> O <sub>3</sub> –CaO system in 1 120°C and 1 200°C.	Slag Atlas <sup>58</sup> *
X	X		X			Pseudobinaries: FeO <sub>x</sub> –SiO <sub>2</sub> (in eq. with met. Fe; in air).	Slag Atlas <sup>58</sup> *
X	X		X			Ternary: Liquidus projection for FeO–Fe <sub>2</sub> O <sub>3</sub> –SiO <sub>2</sub> system.	Slag Atlas <sup>58</sup> *
X	X			X		Pseudobinaries: FeO <sub>x</sub> –MgO (in eq. with met. Fe; in air).	Slag Atlas <sup>58</sup> *
X	X			X		Ternaries: Liquidus projection for FeO–Fe <sub>2</sub> O <sub>3</sub> –MgO system. /Iso-T sections for FeO–Fe <sub>2</sub> O <sub>3</sub> –MgO system in 1 300°C, 1 600°C and 1 750°C.	Slag Atlas <sup>58</sup> *
X	X			X		Iso-T: X(Mg)–p(O <sub>2</sub> ) for 1 000°C.	Slag Atlas <sup>58</sup> *
X	X				X	Pseudobinaries: FeO <sub>x</sub> –Al <sub>2</sub> O <sub>3</sub> (in eq. with met. Fe; in air; in pure oxygen).	Slag Atlas <sup>58</sup> *
X	X				X	Ternary: Liquidus projection for FeO–Fe <sub>2</sub> O <sub>3</sub> –Al <sub>2</sub> O <sub>3</sub> system.	Slag Atlas <sup>58</sup> *
X	X				X	Iso-T: X(Fe)–p(O <sub>2</sub> ) for 1 280°C, 1 380°C and 1 500°C.	Slag Atlas <sup>58</sup> *
X		X	X			<i>cf.</i> quaternary FeO–Fe <sub>2</sub> O <sub>3</sub> –CaO–SiO <sub>2</sub> system.***	Slag Atlas <sup>58</sup> *
X		X		X		<i>cf.</i> quaternary FeO–Fe <sub>2</sub> O <sub>3</sub> –CaO–MgO system.***	Slag Atlas <sup>58</sup> *
X		X			X	<i>cf.</i> quaternary FeO–Fe <sub>2</sub> O <sub>3</sub> –CaO–Al <sub>2</sub> O <sub>3</sub> system.***	Slag Atlas <sup>58</sup> *
X			X	X		<i>cf.</i> quaternary FeO–Fe <sub>2</sub> O <sub>3</sub> –SiO <sub>2</sub> –MgO system.***	Slag Atlas <sup>58</sup> *
X			X		X	<i>cf.</i> quaternary FeO–Fe <sub>2</sub> O <sub>3</sub> –SiO <sub>2</sub> –Al <sub>2</sub> O <sub>3</sub> system.***	Slag Atlas <sup>58</sup> *
X				X	X	<i>cf.</i> quaternary FeO–Fe <sub>2</sub> O <sub>3</sub> –MgO–Al <sub>2</sub> O <sub>3</sub> system.***	Slag Atlas <sup>58</sup> *
	X	X	X			<i>cf.</i> quaternary FeO–Fe <sub>2</sub> O <sub>3</sub> –CaO–SiO <sub>2</sub> system.***	Slag Atlas <sup>58</sup> *
	X	X		X		<i>cf.</i> quaternary FeO–Fe <sub>2</sub> O <sub>3</sub> –CaO–MgO system.***	Slag Atlas <sup>58</sup> *
	X	X			X	<i>cf.</i> quaternary FeO–Fe <sub>2</sub> O <sub>3</sub> –CaO–Al <sub>2</sub> O <sub>3</sub> system.***	Slag Atlas <sup>58</sup> *
	X		X	X		<i>cf.</i> quaternary FeO–Fe <sub>2</sub> O <sub>3</sub> –SiO <sub>2</sub> –MgO system.***	Slag Atlas <sup>58</sup> *
	X		X		X	<i>cf.</i> quaternary FeO–Fe <sub>2</sub> O <sub>3</sub> –SiO <sub>2</sub> –Al <sub>2</sub> O <sub>3</sub> system.***	Slag Atlas <sup>58</sup> *
	X			X	X	<i>cf.</i> quaternary FeO–Fe <sub>2</sub> O <sub>3</sub> –MgO–Al <sub>2</sub> O <sub>3</sub> system.***	Slag Atlas <sup>58</sup> *
		X	X	X		Pseudobinary: MS–CMS <sub>2</sub> .	Slag Atlas <sup>58</sup> *
		X	X	X		Ternaries: Liquidus and solidus projections for CaO–MgO–SiO <sub>2</sub> system.	Slag Atlas <sup>58</sup> *
		X	X		X	Ternary: Liquidus projection for Al <sub>2</sub> O <sub>3</sub> –CaO–SiO <sub>2</sub> system.	Slag Atlas <sup>58</sup> *
		X		X	X	Ternary: Liquidus projection for CaO–MgO–Al <sub>2</sub> O <sub>3</sub> system.	Slag Atlas <sup>58</sup> *
		X		X	X	Ternary: Liquidus projection for CaO–MgO–Al <sub>2</sub> O <sub>3</sub> system.	Ohta and Suito <sup>59</sup> )
			X	X	X	Ternaries: Liquidus projection for Al <sub>2</sub> O <sub>3</sub> –MgO–SiO <sub>2</sub> system. /Iso-T sections for Al <sub>2</sub> O <sub>3</sub> –MgO–SiO <sub>2</sub> system in 1 350°C, 1 450°C and 1 470°C.	Slag Atlas <sup>58</sup> *
<b>Quaternary subsystems</b>							
X	X	X	X			Pseudobinaries: CS–“WS”; C <sub>2</sub> S–W <sub>2</sub> S.	Slag Atlas <sup>58</sup> *
X	X	X	X			Pseudoternaries: Liquidus projection for FeO <sub>x</sub> –CaO–SiO <sub>2</sub> system (in eq. with met. Fe; in air). /Iso-T section for FeO <sub>x</sub> –CaO–SiO <sub>2</sub> system in 1 230°C (in air). /Iso-T sections for FeO–Fe <sub>2</sub> O <sub>3</sub> –CaO plane in 1 450°C and 1 550°C with different SiO <sub>2</sub> contents (0, 5, 10, 20, 30 mass%). /Iso-T section for FeO–Fe <sub>2</sub> O <sub>3</sub> –C <sub>2</sub> S system in 1 500°C.	Slag Atlas <sup>58</sup> *
X	X	X	X			Pseudoternaries: IsoT sections for Fe <sub>2</sub> O <sub>3</sub> –CaO–SiO <sub>2</sub> system in 1 240°C, 1 255°C, 1 270°C and 1 300°C (in air).	Pownceby <i>et al.</i> <sup>60</sup> )

X	X	X	X		Pseudoternaries: IsoT sections for Fe <sub>2</sub> O <sub>3</sub> -CaO-SiO <sub>2</sub> system in 1 240°C, 1 255°C, 1 270°C and 1 300°C (in p(O <sub>2</sub> ) 5·10 <sup>-3</sup> atm).	Pownceby and Clout <sup>61)</sup>
X	X	X	X		Pseudoternaries: IsoT sections for FeO <sub>x</sub> -CaO-SiO <sub>2</sub> system in 1 573 K (in p(O <sub>2</sub> ) 2.1·10 <sup>-3</sup> , 1.8·10 <sup>-6</sup> and 1.8·10 <sup>-8</sup> atm).	Kimura <i>et al.</i> <sup>62)</sup>
X	X	X	X		Pseudoternaries: IsoT sections for FeO-CaO-SiO <sub>2</sub> and Fe <sub>3</sub> O <sub>4</sub> -CaO-SiO <sub>2</sub> systems in 1 573 K (in p(O <sub>2</sub> ) 10 <sup>-9</sup> , 10 <sup>-8</sup> , 10 <sup>-7</sup> , 10 <sup>-6</sup> , 10 <sup>-5</sup> and 3.63·10 <sup>-4</sup> atm). Liquidus projection for Fe <sub>3</sub> O <sub>4</sub> -CaO-SiO <sub>2</sub> system in p(O <sub>2</sub> ) 10 <sup>-6</sup> atm.	Henao <i>et al.</i> <sup>63)</sup>
X	X	X	X		Pseudoternaries: Liquidus projections for FeO <sub>x</sub> -CaO-SiO <sub>2</sub> system in 1 523 K and 1 573 K (in p(O <sub>2</sub> ) from 1.8·10 <sup>-8</sup> to 0.21 atm).	Matsuura <i>et al.</i> <sup>64)</sup>
X	X	X	X		Pseudoternaries: IsoT sections for Fe <sub>3</sub> O <sub>4</sub> -CaO-SiO <sub>2</sub> system in 1 300°C (in p(O <sub>2</sub> ) 10 <sup>-7</sup> atm).	Shigaki <i>et al.</i> <sup>65)</sup>
X	X	X	X		Pseudoternaries: Liquidus and solidus projections for FeO-CaO-SiO <sub>2</sub> system (in p(O <sub>2</sub> ) 10 <sup>-6</sup> atm).	Nikolic <i>et al.</i> <sup>66,67)</sup>
X	X	X	X		Pseudoternaries: Liquidus projections for FeO-CaO-SiO <sub>2</sub> system (in p(O <sub>2</sub> ) 10 <sup>-7</sup> , 10 <sup>-6</sup> and 10 <sup>-5</sup> atm). /Iso-T sections for FeO-CaO-SiO <sub>2</sub> system in 1 200°C and 1 300°C (in p(O <sub>2</sub> ) 10 <sup>-7</sup> and 10 <sup>-5</sup> atm).	Hidayat <i>et al.</i> <sup>68)</sup>
X	X	X		X	Pseudoternaries: Liquidus projection for FeO <sub>x</sub> -MgO-CaO system (in air; in eq. with met. Fe). /Iso-T sections for FeO <sub>x</sub> -MgO-CaO system in 1 500°C (in air; in p(O <sub>2</sub> ) 10 <sup>-3</sup> atm) and 1 600°C (in eq. with met. Fe). /Liquidus projections for FeO-Fe <sub>2</sub> O <sub>3</sub> -MgO plane with different CaO contents (0, 10, 20 mass%).	Slag Atlas <sup>58)</sup> *
X	X	X		X	Quaternaries: Liquidus projection for FeO-Fe <sub>2</sub> O <sub>3</sub> -MgO-CaO system in 1 500°C and 1 600°C. /Iso-T section for FeO-Fe <sub>2</sub> O <sub>3</sub> -MgO-CaO system in 1 500°C (in p(O <sub>2</sub> ) 10 <sup>-3</sup> atm).	Slag Atlas <sup>58)</sup> *
X	X	X		X	Pseudoternaries: Liquidus projection for FeO <sub>x</sub> -Al <sub>2</sub> O <sub>3</sub> -CaO system (in air; in p(O <sub>2</sub> ) 10 <sup>-5</sup> and 10 <sup>-8</sup> atm). /Iso-T sections for FeO <sub>x</sub> -Al <sub>2</sub> O <sub>3</sub> -CaO system in 1 170°C and 1 170°C (in air) and 1 600°C (in eq. with met. Fe).	Slag Atlas <sup>58)</sup> *
X	X		X	X	Pseudoternaries: Liquidus projections for FeO <sub>x</sub> -MgO-SiO <sub>2</sub> system (in eq. with met. Fe; in air; in pure oxygen). /Solidus projection for FeO <sub>x</sub> -MgO-SiO <sub>2</sub> system. /Solubility limits of solid phases for FeO-Fe <sub>2</sub> O <sub>3</sub> -MgO plane in 1 600°C with different SiO <sub>2</sub> contents (0, 10, 16, 23 mass%).	Slag Atlas <sup>58)</sup> *
X	X		X	X	Quaternaries: Liquidus projection for FeO-Fe <sub>2</sub> O <sub>3</sub> -MgO-SiO <sub>2</sub> system in 1 600°C.	Slag Atlas <sup>58)</sup> *
X	X		X	X	Pseudoternaries: Liquidus projections for FeO-MgO-SiO <sub>2</sub> system (in eq. with met. Fe).	Chen <i>et al.</i> <sup>69)</sup>
X	X		X	X	Pseudoternaries: Liquidus projections for FeO-MgO-SiO <sub>2</sub> system (in eq. with met. Fe). /Iso-T sections for FeO-MgO-SiO <sub>2</sub> system in 1 573 K, 1 673 K, 1 773 K, 1 823 K, 1 848 K and 1 873 K (in eq. with met. Fe).	Chen <i>et al.</i> <sup>70)</sup>
X	X		X	X	Pseudobinary: M <sub>2</sub> S-W <sub>2</sub> S.	Chen <i>et al.</i> <sup>70)</sup>
X	X		X	X	Pseudoternaries: Liquidus projection for FeO <sub>x</sub> -Al <sub>2</sub> O <sub>3</sub> -SiO <sub>2</sub> system (in air; in eq. with met. Fe). /Solidus projection for Fe <sub>2</sub> O <sub>3</sub> -Al <sub>2</sub> O <sub>3</sub> -SiO <sub>2</sub> system (in air).	Slag Atlas <sup>58)</sup> *
X	X		X	X	Pseudoternary: MgO solid solution stability region in Al <sub>2</sub> O <sub>3</sub> -Fe <sub>2</sub> O <sub>3</sub> -MgO system in 1 400°C and 1 700°C.	Slag Atlas <sup>58)</sup> *
X		X	X	X	<i>cf.</i> quinary FeO-Fe <sub>2</sub> O <sub>3</sub> -CaO-SiO <sub>2</sub> -MgO system.****	Slag Atlas <sup>58)</sup> *
X		X	X	X	<i>cf.</i> quinary FeO-Fe <sub>2</sub> O <sub>3</sub> -CaO-SiO <sub>2</sub> -Al <sub>2</sub> O <sub>3</sub> system.****	Slag Atlas <sup>58)</sup> *
X		X	X	X	<i>cf.</i> quinary FeO-Fe <sub>2</sub> O <sub>3</sub> -CaO-MgO-Al <sub>2</sub> O <sub>3</sub> system.****	Slag Atlas <sup>58)</sup> *
	X	X	X	X	<i>cf.</i> quinary FeO-Fe <sub>2</sub> O <sub>3</sub> -CaO-SiO <sub>2</sub> -MgO system.****	Slag Atlas <sup>58)</sup> *
	X	X	X	X	<i>cf.</i> quinary FeO-Fe <sub>2</sub> O <sub>3</sub> -CaO-SiO <sub>2</sub> -Al <sub>2</sub> O <sub>3</sub> system.****	Slag Atlas <sup>58)</sup> *
	X	X	X	X	<i>cf.</i> quinary FeO-Fe <sub>2</sub> O <sub>3</sub> -CaO-MgO-Al <sub>2</sub> O <sub>3</sub> system.****	Slag Atlas <sup>58)</sup> *
		X	X	X	Pseudoternaries: Liquidus projections for CaO-MgO-SiO <sub>2</sub> plane with different Al <sub>2</sub> O <sub>3</sub> contents (5, 10, 15, 20, 25, 30, 35 mass%). /Liquidus projections for Al <sub>2</sub> O <sub>3</sub> -CaO-SiO <sub>2</sub> plane with different MgO contents (5, 10, 15 mass%). /Liquidus projections for Al <sub>2</sub> O <sub>3</sub> -CaO-MgO plane with different SiO <sub>2</sub> contents (34, 35, 36, 37 mass%). /Boundaries of primary crystallization fields of solid phases with varying MgO contents.	Slag Atlas <sup>58)</sup> *
		X	X	X	Pseudobinaries: (C+S)-M with 15 and 20 mass% of A for C/S ratios of 1.1 and 1.3. /((C+S)-A with 5 and 10 mass% of M for C/S ratios of 1.1 and 1.3.	Ma <i>et al.</i> <sup>71,72)</sup>
		X	X	X	Pseudoternaries: Liquidus projection for (CaO+SiO <sub>2</sub> )-MgO-Al <sub>2</sub> O <sub>3</sub> plane with C/S ratios of 1.1 and 1.3.	Ma <i>et al.</i> <sup>71,72)</sup>
		X	X	X	Pseudoternaries: Liquidus projections for CaO-MgO-SiO <sub>2</sub> plane with different Al <sub>2</sub> O <sub>3</sub> contents (15, 20 mass%).	Sun <i>et al.</i> <sup>73)</sup>
		X	X	X	Pseudoternary: Liquidus projection for CaO-MgO-SiO <sub>2</sub> plane with 30 mass% Al <sub>2</sub> O <sub>3</sub> .	Gran <i>et al.</i> <sup>74)</sup>
Quinary subsystems						
X	X	X	X	X	Pseudoternaries: Liquidus projections for MgO-Fe <sub>2</sub> O <sub>3</sub> -C <sub>2</sub> S, MgO-C <sub>2</sub> S-C <sub>2</sub> F and MF-C <sub>2</sub> S-C <sub>2</sub> F planes. /Boundaries of primary crystallization fields of solid phases in various subsystem sections.	Slag Atlas <sup>58)</sup> *
X	X	X	X	X	Pseudoquaternary: Liquidus projection for FeO <sub>x</sub> -CaO-MgO-SiO <sub>2</sub> system in 1 600°C in eq. with met. Fe.	Slag Atlas <sup>58)</sup> *
X	X	X	X	X	Pseudoternaries: Liquidus projections for CaO-SiO <sub>2</sub> -FeO <sub>x</sub> -MgO system in 1 573 K (in p(O <sub>2</sub> ) 1.8·10 <sup>-8</sup> , 1.8·10 <sup>-6</sup> and 2.1·10 <sup>-3</sup> atm) with 5 mass% MgO.	Kimura <i>et al.</i> <sup>75)</sup>

X	X	X	X	X		Pseudoternary: Iso-T section for FeO <sub>x</sub> -CaO-SiO <sub>2</sub> plane with 0 and 5 mass% MgO in 1 573 K (in p(O <sub>2</sub> ) 2.7·10 <sup>-7</sup> atm).	Hayashi <i>et al.</i> <sup>76)</sup>
X	X	X	X	X		Pseudoquaternary: Conceptual illustration of liquid-magnetite tie lines in FeO <sub>x</sub> -CaO-MgO-SiO <sub>2</sub> system in 1 573 K (in p(O <sub>2</sub> ) 2.7·10 <sup>-7</sup> atm).	Hayashi <i>et al.</i> <sup>76)</sup>
X	X	X	X		X	Pseudoternaries: Liquidus projections for FeO <sub>x</sub> -Al <sub>2</sub> O <sub>3</sub> -CaO-SiO <sub>2</sub> system with different iron contents (calculated as FeO): 5, 10, 15, 20, 25, 30 mass%. /Liquidus projections for FeO <sub>x</sub> -Al <sub>2</sub> O <sub>3</sub> -CaO-SiO <sub>2</sub> system (in air) with different Fe <sub>2</sub> O <sub>3</sub> contents (10, 16.5, 20 mass%).	Slag Atlas <sup>58)</sup> *
X	X	X	X		X	Pseudoternary: Liquidus projection for Fe <sub>3</sub> O <sub>4</sub> -Al <sub>2</sub> O <sub>3</sub> -CaO-SiO <sub>2</sub> system (in p(O <sub>2</sub> ) 10 <sup>-7</sup> atm) with 5 mass% Al <sub>2</sub> O <sub>3</sub> .	Shigaki <i>et al.</i> <sup>65)</sup>
X	X	X	X		X	Pseudoternaries: Liquidus projections for CaO-SiO <sub>2</sub> -FeO <sub>x</sub> -Al <sub>2</sub> O <sub>3</sub> system in 1 573 K (in p(O <sub>2</sub> ) 1.8·10 <sup>-8</sup> , 1.8·10 <sup>-6</sup> and 2.1·10 <sup>-3</sup> atm) with 5 mass% Al <sub>2</sub> O <sub>3</sub> .	Kimura <i>et al.</i> <sup>75)</sup>
X	X	X	X		X	Pseudoternaries: Liquidus projections for CaO-SiO <sub>2</sub> -FeO <sub>x</sub> -Al <sub>2</sub> O <sub>3</sub> system in 1 573 K (in p(O <sub>2</sub> ) 2.5·10 <sup>-6</sup> , 1.0·10 <sup>-4</sup> and 1.0·10 <sup>-2</sup> atm) with 2 mass% Al <sub>2</sub> O <sub>3</sub> .	Katahira <i>et al.</i> <sup>77)</sup>
X	X	X		X	X	-	-
X	X		X	X	X	Pseudobinaries: (M+W)-S with 2 and 3 mass% A and M/W ratios of 1.2, 1.4, 1.6, 1.8, 2.0 and 2.2.	Chen <i>et al.</i> <sup>78)</sup>
X	X		X	X	X	Pseudoternaries: Liquidus projections for FeO-MgO-SiO <sub>2</sub> plane with 2 and 3 mass% Al <sub>2</sub> O <sub>3</sub> (in eq. with met. Fe). /Iso-T sections for FeO-MgO-SiO <sub>2</sub> plane with 2 and 3 mass% of Al <sub>2</sub> O <sub>3</sub> in 1 773 and 1 823 K.	Chen <i>et al.</i> <sup>78)</sup>
X		X	X	X	X	<i>cf.</i> complete FeO-Fe <sub>2</sub> O <sub>3</sub> -CaO-SiO <sub>2</sub> -Al <sub>2</sub> O <sub>3</sub> -MgO system.*****	Slag Atlas <sup>58)</sup> *
	X	X	X	X	X	<i>cf.</i> complete FeO-Fe <sub>2</sub> O <sub>3</sub> -CaO-SiO <sub>2</sub> -Al <sub>2</sub> O <sub>3</sub> -MgO system.*****	Slag Atlas <sup>58)</sup> *
Complete system with all six components							
X	X	X	X	X	X	Pseudoternaries: Liquidus projections for CaO-SiO <sub>2</sub> -FeO <sub>x</sub> -Al <sub>2</sub> O <sub>3</sub> -MgO system in 1 573 K (in p(O <sub>2</sub> ) 1.8·10 <sup>-8</sup> , 1.8·10 <sup>-6</sup> and 2.1·10 <sup>-3</sup> atm) with 2.5 mass% Al <sub>2</sub> O <sub>3</sub> and 2.5 mass% MgO.	Yajima <i>et al.</i> <sup>79)</sup>
X	X	X	X	X	X	Pseudobinaries: (C+S)-W with 0, 5 and 10 mass% M; 10, 15 and 20 mass% A and C/S ratio of 1.3. / (C+S)-A with 5 and 10 mass% M; 0, 5, 10, 15 and 20 mass% W and C/S ratio of 1.3. / (C+S)-M with 10, 15 and 20 mass% A; 0, 5, 10, 15 and 20 mass% W and C/S ratio of 1.3.	Jang <i>et al.</i> <sup>80,81)</sup>
X	X	X	X	X	X	Pseudoternaries: Liquidus projections for (CaO+SiO <sub>2</sub> )-MgO-Al <sub>2</sub> O <sub>3</sub> plane with 5, 10, 15 and 20 mass% of "FeO" and C/S ratio of 1.3. / Iso-T section for (CaO+SiO <sub>2</sub> )-MgO-Al <sub>2</sub> O <sub>3</sub> plane with 0, 10 and 20 mass% of "FeO" and C/S ratio of 1.3 in 1 723 K.	Jang <i>et al.</i> <sup>80,81)</sup>

\* *cf.* Slag Atlas<sup>58)</sup> for the list of references to the original articles, from which the diagrams in Slag Atlas<sup>58)</sup> were constructed.

\*\* Binaries of FeO-X and Fe<sub>2</sub>O<sub>3</sub>-X (in which X refers to either CaO, SiO<sub>2</sub>, MgO or Al<sub>2</sub>O<sub>3</sub>) are not included in Slag Atlas<sup>58)</sup> because all the "binary" systems containing iron oxide(s) are actually pseudobinary diagrams in the form of FeO<sub>x</sub>-X with a fixed state of oxidation (*e.g.* in equilibrium with metallic iron, in equilibrium with air or in equilibrium with oxygen).

\*\*\* Ternaries of FeO-X-Y and Fe<sub>2</sub>O<sub>3</sub>-X-Y (in which X and Y refer to either CaO, SiO<sub>2</sub>, MgO or Al<sub>2</sub>O<sub>3</sub>) are not included in Slag Atlas<sup>58)</sup> because all the "ternary" systems containing iron oxide(s) are actually pseudoternary diagrams in the form of FeO<sub>x</sub>-X-Y with a fixed state of oxidation (*e.g.* in equilibrium with metallic iron, in equilibrium with air or in equilibrium with oxygen).

\*\*\*\* Quaternaries of FeO-X-Y-Z and Fe<sub>2</sub>O<sub>3</sub>-X-Y-Z (in which X, Y and Z refer to either CaO, SiO<sub>2</sub>, MgO or Al<sub>2</sub>O<sub>3</sub>) are not included in Slag Atlas<sup>58)</sup> because all the "quaternary" systems containing iron oxide(s) are actually pseudoquaternary diagrams in the form of FeO<sub>x</sub>-X-Y-Z with a fixed state of oxidation (*e.g.* in equilibrium with metallic iron, in equilibrium with air or in equilibrium with oxygen).

\*\*\*\*\* Quinaries of FeO-CaO-SiO<sub>2</sub>-MgO-Al<sub>2</sub>O<sub>3</sub> and Fe<sub>2</sub>O<sub>3</sub>-CaO-SiO<sub>2</sub>-MgO-Al<sub>2</sub>O<sub>3</sub> are not included in Slag Atlas<sup>58)</sup> because all the "quinary" systems containing iron oxide(s) are actually pseudoquinary diagrams in the form of FeO<sub>x</sub>-CaO-SiO<sub>2</sub>-MgO-Al<sub>2</sub>O<sub>3</sub> with a fixed state of oxidation (*e.g.* in equilibrium with metallic iron, in equilibrium with air or in equilibrium with oxygen). Unlike for lower degree subsystems, there is no phase diagrams for the complete FeO-Fe<sub>2</sub>O<sub>3</sub>-CaO-SiO<sub>2</sub>-MgO-Al<sub>2</sub>O<sub>3</sub> system in Slag Atlas<sup>58)</sup> However, this system is studied by Yajima *et al.*<sup>79)</sup>

In complex compounds, A, C, F, M, S and W refer to Al<sub>2</sub>O<sub>3</sub>, CaO, Fe<sub>2</sub>O<sub>3</sub>, MgO, SiO<sub>2</sub> and FeO, respectively.

to its importance in formation of bonding SFCA phases as explained in chapter 2.2.2.

As mentioned in chapter 2, the raw material undergoes various stages with different temperatures and partial pressures of oxygen during the sintering process. During this cycle, primary hematite is partly reduced into magnetite and then oxidized back into secondary hematite, whereas initial melt rich in CaO and SiO<sub>2</sub> is formed and reacts with hematite to form ferritic bonding phases such as SFC (silico-ferrite of calcia) solid solutions. In a stage with the highest temperature and the most reducing conditions, the amounts of magnetite and silicate liquid phase are the highest, whereas the amounts of hematite and SFC are smaller. During the cooling stage, the liquid solidifies to form both crystalline as well as glassy, amorphous phases.<sup>61)</sup>

In order to define the conditions needed to maximize the stability of SFC solid solution, which - in turn - is related

to the formation of the SFCA (silico-ferrite of calcium and aluminium) needed as a bonding phase in sinters, the iron-rich area of the FeO<sub>x</sub>-CaO-SiO<sub>2</sub> system needs to be understood.<sup>47,60,61,153-155)</sup> Experimentally determined phase equilibria of this system in the conditions of the sintering process have been illustrated by *e.g.* Pownceby and Clout.<sup>61)</sup> In their paper<sup>61)</sup> they aimed to extend their previous studies of the same system in atmospheric pressures<sup>60)</sup> to obtain a more accurate view on the formation of different phases during the heating stage of the sintering process, in which partial pressure of oxygen is decreased to the magnitude of 10<sup>-3</sup> atm<sup>32,33)</sup> due to the combustion of coke particles (after which the partial pressure of oxygen once again increases during the cooling stage).<sup>61)</sup> Temperature range in both of their studies was chosen to be between 1 240°C and 1 300°C.<sup>60,61)</sup>

From the isothermal sections (from 1 240°C to 1 300°C) of the pseudoternary Fe<sub>2</sub>O<sub>3</sub>-CaO-SiO<sub>2</sub> system in air pre-

**Table 6.** A list of studies, in which assessment and optimization of thermochemical data has been done for the systems containing FeO, Fe<sub>2</sub>O<sub>3</sub>, CaO, SiO<sub>2</sub>, MgO and/or Al<sub>2</sub>O<sub>3</sub>.

Components						Solution models					Software	Reference	
FeO	Fe <sub>2</sub> O <sub>3</sub>	CaO	SiO <sub>2</sub>	MgO	Al <sub>2</sub> O <sub>3</sub>	Method	(Mod.) Quasi-chem. model (MQM)	Two- sublattice model for ionic liq. (RILM)	Sublattice model (based on CEF)	Polynom. model			Others
Binary subsystems													
X	X					CALPHAD	Liquid		Spinel	Monoxide		FACT	Decterov <i>et al.</i> <sup>82)</sup>
X	X					CALPHAD	Liquid					FACT	Hidayat <i>et al.</i> <sup>83)</sup>
X	X					CALPHAD							Spencer and Kubaschewski <sup>84)</sup>
X	X					CALPHAD		Liquid	Solid sol.			TC	Sundman <sup>85)</sup>
X	X					CALPHAD		Liquid	Solid sol.			TC	Fabrichnaya and Sundman <sup>86)</sup>
X		X				CALPHAD	Liquid					FACT	Pelton and Blander <sup>87)</sup>
X		X				CALPHAD	Liquid					FACT	Wu <i>et al.</i> <sup>88)</sup>
X			X			CALPHAD	Liquid					FACT	Pelton and Blander <sup>87)</sup>
X			X			CALPHAD	Liquid					FACT	Wu <i>et al.</i> <sup>89)</sup>
X				X		CALPHAD	Liquid					FACT	Wu <i>et al.</i> <sup>88)</sup>
X				X		CALPHAD	Liquid					FACT	Wu <i>et al.</i> <sup>89)</sup>
X					X	CALPHAD	Liquid				Regular (Spinel)	FACT	Eriksson <i>et al.</i> <sup>90)</sup>
		X	X			CALPHAD					Cell model	MPE	Taylor and Dinsdale <sup>91)</sup>
		X	X			CALPHAD	Liquid					FACT	Pelton and Blander <sup>87)</sup>
		X	X			CALPHAD		Liquid	Solid sol.			TC	Hillert <i>et al.</i> <sup>92)</sup>
		X	X			CALPHAD		Liquid	Solid sol.			TC	Huang <i>et al.</i> <sup>93)</sup>
		X		X		CALPHAD		Liquid					Zhang and Yong <sup>94)</sup>
		X		X		CALPHAD	Liquid	Liquid	Solid sol.			TC	Huang <i>et al.</i> <sup>93)</sup>
		X		X		CALPHAD						FACT	Wu <i>et al.</i> <sup>88)</sup>
		X		X		CALPHAD						FACT	Blander and Pelton <sup>95)</sup>
		X			X	CALPHAD	Liquid					FACT	Eriksson and Pelton <sup>96)</sup>
		X			X	CALPHAD					Cell model	MPE	Zhang <i>et al.</i> <sup>97)</sup>
		X			X	CALPHAD		Liquid				TC	Mao <i>et al.</i> <sup>98)</sup>
		X			X	CALPHAD		Liquid				TC	Hallstedt <sup>99)</sup>
			X	X		CALPHAD		Liquid	Solid sol.			TC	Huang <i>et al.</i> <sup>93)</sup>
			X	X		CALPHAD	Liquid					FACT	Wu <i>et al.</i> <sup>89)</sup>
			X	X		CALPHAD	Liquid					FACT	Blander and Pelton <sup>95)</sup>
				X	X	CALPHAD	Liquid					FACT	Eriksson and Pelton <sup>96)</sup>
				X	X	CALPHAD					Cell model	MPE	Zhang <i>et al.</i> <sup>97)</sup>
				X	X	CALPHAD		Liquid	Solid sol.			TC	Zienert and Fabrichnaya <sup>100)</sup>
				X	X	CALPHAD		Liquid				TC	Mao <i>et al.</i> <sup>98)</sup>
				X	X	CALPHAD		Liquid	Solid sol.			TC	Hallstedt <sup>101)</sup>
				X	X	CALPHAD	Liquid		Spinel, monoxide, pyroxene			FACT	Jung <i>et al.</i> <sup>102)</sup>
Ternary subsystems													
X	X	X				CALPHAD		Liquid	Solid sol.			TC	Hillert <i>et al.</i> <sup>103)</sup>
X	X	X				CALPHAD	Liquid		Spinel		Bragg–Williams (Monox.)	FACT	Hidayat <i>et al.</i> <sup>104)</sup>
X	X		X			CALPHAD	Liquid					FACT	Hidayat <i>et al.</i> <sup>105)</sup>
X	X		X			CALPHAD		Liquid	Solid sol.			TC	Fabrichnaya and Sundman <sup>86)</sup>
X	X			X		CALPHAD	Liquid		Spinel, Olivine, Pyroxene, Monoxide			FACT	Jung <i>et al.</i> <sup>106)</sup>
X	X				X	CALPHAD		Liquid	Solid sol.			TC	Dreval <i>et al.</i> <sup>107)</sup>
X	X				X	CALPHAD	Liquid		Spinel, Mullite			FACT	Prostakova <i>et al.</i> <sup>108)</sup>
X		X	X			CALPHAD	Liquid					FACT	Pelton and Blander <sup>87)</sup>
X		X	X			CALPHAD		Liquid				TC	Hallstedt <i>et al.</i> <sup>109)</sup>
X		X	X			CALPHAD		Liquid				TC	Selleby <sup>110)</sup>

X				X	CALPHAD	Liquid		Solid sol.	Melilite	FACT	Jak <i>et al.</i> <sup>53)</sup>	
X			X	X	CALPHAD				Solid sol.	–	Saxena <sup>111)</sup>	
X			X	X	CALPHAD	Liquid				FACT	Wu <i>et al.</i> <sup>89)</sup>	
X			X	X	CALPHAD	Liquid				FACT	Blander and Pelton <sup>95)</sup>	
X			X		X	CALPHAD	Liquid	Solid sol.	Melilite	FACT	Jak <i>et al.</i> <sup>53)</sup>	
	X	X	X		CALPHAD		Liquid			TC	Hallstedt <i>et al.</i> <sup>109)</sup>	
	X	X	X		CALPHAD		Liquid			TC	Selleby <sup>110)</sup>	
	X	X		X	CALPHAD	Liquid		Solid sol.	Melilite	FACT	Jak <i>et al.</i> <sup>53)</sup>	
	X		X	X	CALPHAD	Liquid		Solid sol.	Melilite	FACT	Jak <i>et al.</i> <sup>53)</sup>	
		X	X	X	CALPHAD		Liquid	Solid sol.		TC	Huang <i>et al.</i> <sup>93)</sup>	
		X	X	X	CALPHAD	Liquid				FACT	Blander and Pelton <sup>95)</sup>	
		X	X	X	CALPHAD	Liquid		Olivine, Pyroxene		FACT	Jung <i>et al.</i> <sup>112)</sup>	
		X	X		X	CALPHAD	Liquid			FACT	Eriksson and Pelton <sup>96)</sup>	
		X	X		X	CALPHAD			Cell model	MPE	Zhang <i>et al.</i> <sup>97)</sup>	
		X		X	X	CALPHAD	Liquid	Spinel, Pyroxene, Monoxide		FACT	Jung <i>et al.</i> <sup>102)</sup>	
			X	X	X	CALPHAD	Liquid	Spinel, Pyroxene, Monoxide		FACT	Jung <i>et al.</i> <sup>102)</sup>	
Quaternary subsystems												
X	X	X	X		CALPHAD		Liquid			TC	Selleby <sup>110)</sup>	
X	X	X	X		CALPHAD				Cell model	MPE	Chen <i>et al.</i> <sup>113)</sup>	
X	X	X	X		CALPHAD	Liquid		Spinel, Olivine, Pyroxene, Melilite	Bragg-Williams (C <sub>2</sub> S)	FACT	Hidayat <i>et al.</i> <sup>114)</sup>	
X	X	X		X	CALPHAD	Liquid		Solid sol.	Melilite	FACT	Jak <i>et al.</i> <sup>53)</sup>	
X	X		X	X	CALPHAD		Liquid	Solid sol.		TC	Fabrichnaya <sup>115)</sup>	
X	X		X	X	CALPHAD			Monoxide	Regular	TC	Fabrichnaya <sup>116)</sup>	
X	X		X	X	CALPHAD	Liquid		Spinel, Olivine, Pyroxene, Monoxide	Bragg-Williams (C <sub>2</sub> S)		Jung <i>et al.</i> <sup>55)</sup>	
X	X		X	X	CALPHAD	Liquid		Spinel, Olivine, Pyroxene, Monoxide	Bragg-Williams (C <sub>2</sub> S)		Dechterov <i>et al.</i> <sup>117)</sup>	
X	X		X	X	CALPHAD	Liquid		Solid sol.	Melilite	FACT	Jak <i>et al.</i> <sup>53)</sup>	
X	X		X	X	CALPHAD	Liquid		Spinel, Mullite		FACT	Prostakova <i>et al.</i> <sup>108)</sup>	
		X	X	X	X	CALPHAD		SFCA		MPE	Chen <i>et al.</i> <sup>47)</sup>	
		X	X	X	X	CALPHAD	Liquid	SFCA		FACT	Murao <i>et al.</i> <sup>11)</sup>	
Quinary subsystems												
X	X	X	X		X	CALPHAD	Liquid	Solid sol.	Melilite	FACT	Jak <i>et al.</i> <sup>53,118)</sup>	
		X	X	X	X	CALPHAD				TC	Tazuddin <i>et al.</i> <sup>52)</sup>	
Complete system with all six components												
X	X	X	X	X	X	CALPHAD		Liquid	Solid sol.	Cell model (Liquid)	TC	Andersson <i>et al.</i> <sup>119)</sup>
X	X	X	X	X	X	CALPHAD			Solid sol.	Associate (Liquid)	MTD	Barry <i>et al.</i> <sup>120)</sup>
X	X	X	X	X	X	CALPHAD	Liquid		Solid sol.		FACT	Dechterov <i>et al.</i> <sup>121)</sup>
X	X	X	X	X	X	CALPHAD	Liquid		Solid sol.	Solid sol.	FACT	Kongoli and Yazawa <sup>122)</sup>
X	X	X	X	X	X	CALPHAD				Cell model (Liquid)	CEQCSI	Gaye <i>et al.</i> <sup>123)</sup>
X	X	X	X	X	X	CALPHAD				GCA (Liquid)	CEQCSI	Lehmann <i>et al.</i> <sup>124,125)</sup>
X	X	X	X	X	X	CALPHAD				GCA (Liquid)	CEQCSI	Lehmann and Zhang <sup>126)</sup>
X	X	X	X	X	X	CALPHAD				Cell model (Liquid)	MPE	Zhang <i>et al.</i> <sup>127)</sup>
X	X	X	X	X	X	CALPHAD				Cell model (Liquid)	MPE	Jahanshahi <i>et al.</i> <sup>128)</sup>

Abbreviations of thermochemical software: CEQCSI = Calcul d'Equilibre Chimique pour la Sidérurgie (Chemical Equilibrium Calculations for the Steel Industry); FACT = FactSage; MPE = Multicomponent Phase Equilibria; MTD = MTDATA; TC = ThermoCalc.

**Table 7.** Possibilities to model phases potentially existing in iron ore sinters with different software.

Name*	Solution phase		Software/models				
	Formula** (if available)	Examples	CEQCSI	FACT	MPE	MTD	TC
Molten oxide phase	Varies	Molten slag phase	CM/GCA	MQM	CM/GCA	AM	CM/AM/ RILM
Monoxide/Halite	X <sup>+II</sup> O	Wüstite, lime, magnesiowüstite	Yes****	CEF	RSM with RKM	CEF	CEF
Spinel	X <sup>+II</sup> Y <sup>+III</sup> <sub>2</sub> O <sub>4</sub>	Magnetite	Yes****	CEF	RSM with RKM	CEF	CEF
Corundum	X <sup>+III</sup> <sub>2</sub> O <sub>3</sub>	Hematite, alumina		CEF	RSM with RKM	CEF	CEF
Olivine	X <sup>+II</sup> <sub>2</sub> SiO <sub>4</sub>	Fayalite, forsterite		CEF	RSM with RKM	CEF	CEF
Pyroxenes	X <sup>+II</sup> Y <sup>+II/+III</sup> Z <sup>+III/+IV</sup> SiO <sub>6</sub>	Hedenbergite	Yes****	CEF	RSM with RKM	CEF	CEF
Garnet	X <sup>+II</sup> <sub>3</sub> Y <sup>+III</sup> <sub>2</sub> Si <sub>3</sub> O <sub>12</sub>	Grossular		CEF			CEF
Melilite	Ca <sub>2</sub> X <sup>+II/+III</sup> Y <sup>+III/+IV</sup> <sub>2</sub> O <sub>7</sub>	Gehlenite, åkermanite	Yes****	CEF	RSM with RKM	CEF	CEF
Cordierite	Al <sub>4</sub> X <sup>+II</sup> <sub>2</sub> Si <sub>5</sub> O <sub>18</sub>			CEF			CEF
Wollastonite	(Ca,X <sup>+II</sup> )SiO <sub>3</sub>			CEF		CEF	CEF
Dicalcium silicate	(Ca,X <sup>+II</sup> ) <sub>2</sub> SiO <sub>4</sub>			CEF		CEF	CEF
SFCA	Varies***			CEF*****	CEF		
Calcium-aluminium-ferrites	Several; cf. examples	C <sub>3</sub> AF, C <sub>2</sub> AF, CAF, CAF <sub>2</sub> , CAF <sub>3</sub> , CAF <sub>6</sub> (C = CaO; A = Al <sub>2</sub> O <sub>3</sub> ; F = Fe <sub>2</sub> O <sub>3</sub> )		CEF			CEF

Abbreviations of thermochemical software: CEQCSI = Calcul d'Equilibre Chimique pour la Sidérurgie (Chemical Equilibrium Calculations for the Steel Industry); FACT = FactSage; MPE = Multicomponent Phase Equilibria; MTD = MTDATA; TC = ThermoCalc.

Abbreviations of thermodynamic models: AM = Associate model; CEF = Sublattice model based on Compound energy formalism; CM = Cell model; GCA = Generalized central atom model; MQM = Modified quasi-chemical model; RILM = Reciprocal ionic liquid model (two-sublattice model for ionic liquids); RKM = Redlich-Kister-Muggianu polynomial (for the excess function); RSM = Regular solution model.

\* Some software may use different names to describe the same phase.

\*\* Possible oxidation states are only mentioned for substitutional elements marked with X, Y and Z. Oxidation states of oxygen, calcium, aluminium and silicon are -II, +II, +III and +IV, respectively.

\*\*\* Concerning the formula of SFCA phases, see chapters 2.2.2 and 4 for more detailed discussion.

\*\*\*\* Models not specified in the documentation.

\*\*\*\*\* SFCA is not mentioned in the documentation of the FactSage's database descriptions, but the assessment of the data for SFCA has been reported by Murao *et al.*<sup>11)</sup>

sented by Pownceby and Clout,<sup>60,61)</sup> it is seen that in the temperatures higher than 1 250°C the main phases of the sinter system are liquid solution as well as solid Fe<sub>3</sub>O<sub>4</sub>, C<sub>2</sub>S and C<sub>2</sub>F, in which C, F and S refer to CaO, Fe<sub>2</sub>O<sub>3</sub> and SiO<sub>2</sub>, respectively. It is also seen that the homogeneous stability region of the liquid phase extends from iron oxide rich area to the silica rich concentrations. However, in temperatures below 1 250°C this liquid region is divided into two regions: one with higher iron oxide content and higher basicity and the other with higher SiO<sub>2</sub> content and lower basicity. As the partial pressure of oxygen is decreased from the atmospheric values, the region of the silicate melt is enlarged significantly in comparison to the calcium ferritic melt. According to the experiments by Pownceby and Clout<sup>61)</sup> in the sintering conditions, the bulk composition of the sinter lies within the three phase region of liquid, magnetite and SFC solid solution. Furthermore, the SFC solid solution, which acts as a major ferritic bonding phase in low-Al<sub>2</sub>O<sub>3</sub> sinters, cannot be formed as a single crystalline phase in these conditions. Combined with their experiments in air,<sup>60)</sup> they concluded that in order to maximise the formation of SFC solid solution in lower temperatures, a semi-reduced heating followed by slow, oxidizing cooling is preferable.<sup>61)</sup>

With an addition of Al<sub>2</sub>O<sub>3</sub> into the studied system, a more comprehensive view on the bonding phase formation can be achieved. As initially presented by Hancart *et al.*<sup>46)</sup> and reported by various other researchers since then, a complex

silico-ferrite of calcium and aluminium (SFCA), which can be represented by the formula xFe<sub>2</sub>O<sub>3</sub>·ySiO<sub>2</sub>·zAl<sub>2</sub>O<sub>3</sub>·5CaO (with x + y + z = 12), is regarded as an essential bonding phase in industrial sinters and must therefore be understood in order to control the sintering process properly<sup>153,154)</sup> (*c.f.* chapter 2.2.2). Pseudoquaternary Fe<sub>2</sub>O<sub>3</sub>-SiO<sub>2</sub>-Al<sub>2</sub>O<sub>3</sub>-CaO diagrams (assuming conditions to be oxidizing enough to stabilize Fe<sub>2</sub>O<sub>3</sub> over Fe<sub>3</sub>O<sub>4</sub> and FeO) can be used to illustrate the substitution mechanisms between different cations in the SFCA solid solution. According to Patrick and Pownceby,<sup>153)</sup> substitution mechanisms and solid solubilities can be shown within a plane in which CF<sub>3</sub>, CA<sub>3</sub> and C<sub>4</sub>S<sub>3</sub> (in which C, F, A and S refer to CaO, Fe<sub>2</sub>O<sub>3</sub>, Al<sub>2</sub>O<sub>3</sub> and SiO<sub>2</sub>, respectively) are chosen as end members. According to their results, the greatest range of solubility occurs in the direction of the Al<sup>3+</sup> ↔ Fe<sup>3+</sup> exchange (between CF<sub>3</sub> and CA<sub>3</sub>), whereas the coupled substitution involving 2 (Al<sup>3+</sup>, Fe<sup>3+</sup>) ↔ (Ca<sup>2+</sup>, Fe<sup>2+</sup>) + Si<sup>4+</sup> (between CF<sub>3</sub> and C<sub>4</sub>S<sub>3</sub>) is not as extensive.<sup>153)</sup> Alternative suggestions as compositional planes, in which substitutions take place, have been proposed by *e.g.* Inoue & Ikeda<sup>156)</sup> (CF<sub>3</sub>, CA<sub>3</sub> and CS<sub>3</sub> as end members) and Dawson *et al.*<sup>157)</sup> (CF<sub>2</sub>, CA<sub>2</sub> and CS<sub>3</sub> as end members).

Patrick and Pownceby<sup>153)</sup> also used CF<sub>3</sub>-CA<sub>3</sub>-C<sub>4</sub>S<sub>3</sub> planes to illustrate, how the substitution decreases and stability region becomes smaller as temperature is increased. Both laboratory experiments and analyses from various samples of industrial sinters suggest that the stability of the SFCA

solid solution is increased with increasing  $\text{Al}_2\text{O}_3$  content and the  $\text{Al}_2\text{O}_3$ -rich SFCA is stable at  $200^\circ\text{C}$  higher temperatures in comparison to alumina-free SFC phase.<sup>153)</sup> The effects of sinter composition (e.g. contents of  $\text{Al}_2\text{O}_3$  and  $\text{TiO}_2$  as well as  $\text{CaO}/\text{SiO}_2$  ratio) and conditions (temperature and partial pressure of oxygen) on the stabilities of SFCA solid solutions, liquid phase as well as other stable phases of the  $\text{FeO}_x$ - $\text{SiO}_2$ - $\text{CaO}$ - $\text{Al}_2\text{O}_3$  system has been studied and described in more detail by Pownceby and Webster and their co-workers in their more recent publications.<sup>19,154,158-162)</sup> Based on their comprehensive experiments and analyses and with the help of illustrative phase diagrams of the studied systems, Webster *et al.*<sup>158)</sup> summarized the flow sheet illustrating the reaction sequences leading into the formation of the SFCA phases (cf. Fig. 1). It should also be noted that although in this chapter it has so far only been referred to one SFCA solid solution, at least three different type of silico-ferrites of calcium and aluminium have been reported in the literature:<sup>11,47)</sup> so-called SFCA-I ( $\text{A}_3\text{B}_8\text{M}_8\text{T}_8\text{O}_{28}$ ) and SFCA-II ( $\text{A}_4\text{T}_{14}\text{M}_{16}\text{O}_{48}$ ) in addition to SFCA ( $\text{A}_2\text{T}_6\text{M}_6\text{O}_{20}$ ), in which A, B, M and T refer  $\text{Ca}^{2+}$ , either  $\text{Ca}^{2+}$  or  $\text{Fe}^{2+}$ , octohedral cation site and tetrahedral cation site, respectively.<sup>11)</sup> The existence of the SFCA and SFCA-I phases has been verified in iron ore sinters,<sup>49)</sup> but it is not known whether SFCA-II is formed in industrial sinters.<sup>42)</sup> From the practical point of view SFCA-I has been considered to be the most desirable bonding phase in sinters because it yields higher strength and better reducibility.<sup>47)</sup> It should also be kept in mind that despite the general chemical formulae presented for SFCA, SFCA-I and SFCA-II phases above, the morphologies of the silico-ferrites of calcium and aluminium are not solely defined by the chemical composition, but are also influenced by other factors such as cooling, melt viscosity and kinetics. As reported in a comprehensive review on the compositions, structures and formation mechanisms of the SFCA phases by Nicol *et al.*,<sup>135)</sup> a wide variety of SFCA morphologies (e.g. acicular, platy, fibrous, irregularly-shaped, needle-like, dendritic, columnar, tabular, blocky, prosmatic, lath-shaped and crystalline, some of which describe similar morphologies with different names defined by different researchers) have been observed and reported by many researchers, and there still is large inconsistency concerning the classification and naming of silico-ferrites of calcium and aluminium.

In order to take the SFCA phases into account in phase stability simulations it is necessary to have accurate assessments of thermochemical data for these phases based on the phase stability experiments and analyses that have been made. This kind of data assessment have been reported within the context of the FactSage software<sup>129-131)</sup> by e.g. Murao *et al.*<sup>11)</sup> and within the context of the MPE software<sup>127,128)</sup> by e.g. Chen *et al.*<sup>47)</sup> A compound energy formalism<sup>143)</sup> with three sublattices has been used to describe the SFCA phase in thermodynamic modelling.<sup>47)</sup>

Finally, once thermochemical data has been assessed for a system including all the major components in sinters, this data can be used not only to study the phenomena during the sintering process, but also to estimate the behaviour of sinter during the reduction processes such as blast furnace. For example, Iljana *et al.*<sup>17,163,164)</sup> have reported a good correspondence between computational results for  $\text{FeO}_x$ - $\text{SiO}_2$ - $\text{CaO}$ - $\text{MgO}$ - $\text{Al}_2\text{O}_3$  system and laboratory experiments when

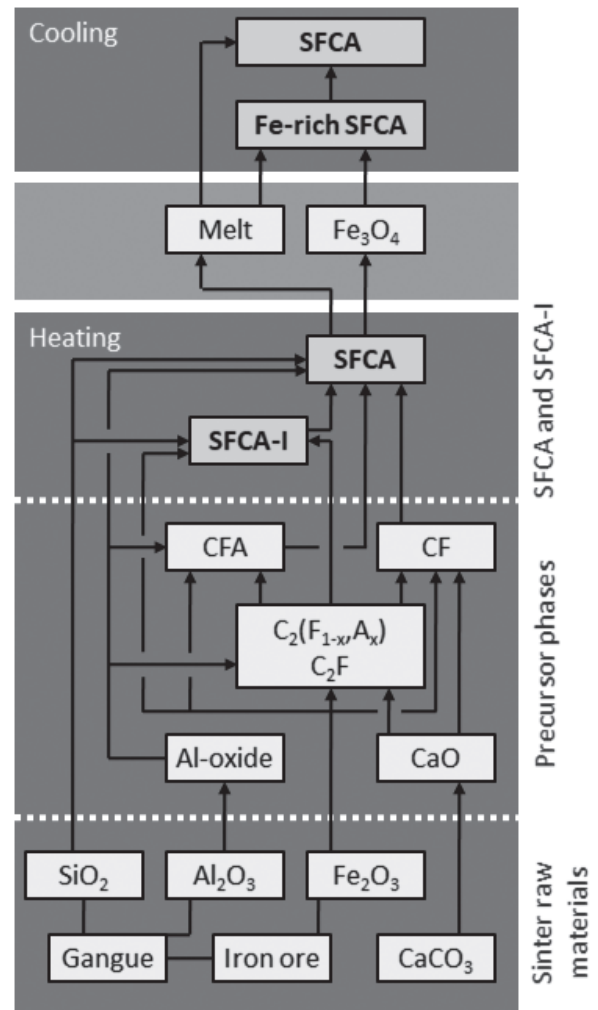


**Fig. 1.** Summary of the reaction sequences in the formation of SFCA-I and SFCA phases during heating and cooling in the range of  $25$ – $1350^\circ\text{C}$  and  $p(\text{O}_2)$  of  $5 \cdot 10^{-3}$  atm. A zone, in which  $\text{Fe}_3\text{O}_4$  and melt coexist, is located between the heating and cooling zones. Heating zone is further divided into three subsections. Based on Webster *et al.*<sup>158)</sup>

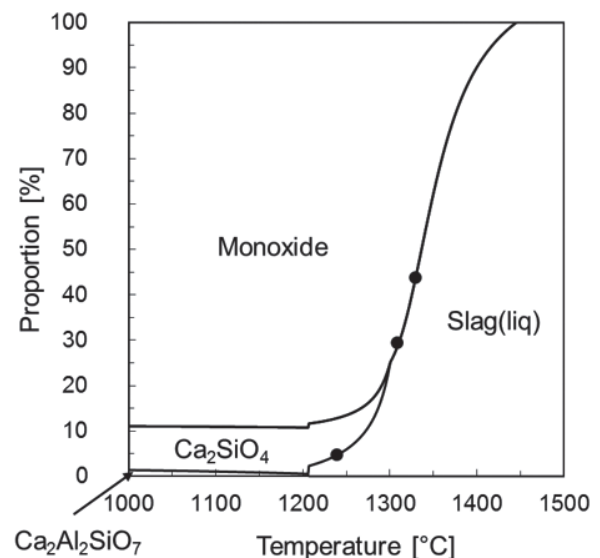


**Fig. 2.** FactSage-computed proportions of the existing phases in the basic sinter as temperature rises in a blast furnace. The experimental estimations of the proportions of the slag phase at the end of the reduction-softening test have been marked with black dots.<sup>17)</sup>

studying the behaviour of sinter in the cohesive zone of a blast furnace as seen from Fig. 2.

## 5. Summary

Sintering process is a commonly used pre-treatment process to manufacture a burden material for the blast furnace. During the sintering process the material undergoes a series of reactions, during which the varying conditions (*i.e.* temperature and state of oxidation) cause changes in the mineralogical composition of the material. The main purpose of the sintering process is to produce porous, agglomerated sinter material with suitable chemical, physical and mechanical properties to be charged into the blast furnace. Although the sintering process is very fast and the material does not fully reach the chemical equilibrium during the process, it is nevertheless important to understand the phase equilibria of the sinter system in order to analyse and control the effect of various factors on the sintering process.

Despite the compositional variations in different sinters, the main components of practically all sinters are FeO, Fe<sub>2</sub>O<sub>3</sub>, SiO<sub>2</sub>, CaO, Al<sub>2</sub>O<sub>3</sub> and MgO, which cover approximately 99% of the sinter chemistry in total. Hence, a reasonable comprehensive view on the behaviour of sinters can be obtained by studying the phase equilibria within this six-component system. Based on the experimental data (*i.e.* phase diagrams, solubilities, *etc.*), oxide databases including all the relevant components - although not necessarily data for all the relevant phases (such as SFCA) - have been created with a CALPHAD method. These databases are commercially available with computational thermochemistry software and can thus be used to compute innumerable amount of phase diagram sections in order to illustrate the phase equilibria within the FeO–Fe<sub>2</sub>O<sub>3</sub>–SiO<sub>2</sub>–CaO–Al<sub>2</sub>O<sub>3</sub>–MgO system. As long as all the relevant data is available in the databases, these computed phase diagrams provide a useful tool to study the behaviour of the material in both sintering process itself as well as in the following reduction processes such as the blast furnace.

## Acknowledgements

The authors wish to thank their colleagues Mr. Pekka Tanskanen and D.Sc. (Tech.) Ville-Valtteri Visuri for fruitful discussions and useful comments concerning the manuscript. The patience and the helpfulness of the personnel of the National Repository Library in Kuopio is also acknowledged with great gratitude.

## Abbreviations

AM: Associate model

BF: Blast furnace

CALPHAD: Calculation of phase diagrams; Computer coupling of phase diagrams and thermochemistry

CEF: Compound energy formalism

CEQCSI: Calcul d'Equilibre Chimique pour la Sidérurgie (Chemical Equilibrium Calculations for the Steel Industry)

CM: Cell model

CSIRO: Commonwealth Scientific and Industrial Research Organisation

EDS: Energy dispersive spectroscopy

EPMA: Electron probe microanalysis

FACT: FactSage

GCA: Generalized central atom model

GTT: GTT-Technologies

IRSID: Institut de Recherché de la Sidérurgie

MPE: Multicomponent Phase Equilibria

MTD: MTDATA

MQM: Modified quasi-chemical model

NPL: National Physical Laboratory

OM: Optical microscopy

RILM: Reciprocal ionic liquid model

RKM: Redlich-Kister-Muggianu polynomial

RSM: Regular solution model

SEM: Scanning electron microscopy

SFC: Silico-ferrite of calcia

SFCA: Silico-ferrite of calcium and aluminium

TC: ThermoCalc

TEM: Transmission electron microscopy

XRD: X-ray diffraction

XRF: X-ray fluorescence

## REFERENCES

- 1) D. Fernández-González, I. Ruiz-Bustinza, J. Mochón, C. González-Gasca and L. F. Verdeja: *Miner. Process. Extr. Metall. Rev.*, **38** (2017), 36. <https://doi.org/10.1080/08827508.2016.1244059>
- 2) D. Fernández-González, I. Ruiz-Bustinza, J. Mochón, C. González-Gasca and L. F. Verdeja: *Miner. Process. Extr. Metall. Rev.*, **38** (2017), 215. <https://doi.org/10.1080/08827508.2017.1288115>
- 3) D. Fernández-González, I. Ruiz-Bustinza, J. Mochón, C. González-Gasca and L. F. Verdeja: *Miner. Process. Extr. Metall. Rev.*, **38** (2017), 254. <https://doi.org/10.1080/08827508.2017.1323744>
- 4) T. C. Eisele and S. K. Kawatra: *Miner. Process. Extr. Metall. Rev.*, **24** (2003), 1. <https://doi.org/10.1080/08827500306896>
- 5) L. Lu and O. Ishiyama: *Iron Ore*, ed. by L. Lu, Woodhead Publishing, Cambridge, UK, (2015), 395. <https://doi.org/10.1016/B978-1-78242-156-6.00014-9>
- 6) R. A. Kravchenko, G. S. Vasil'ev and N. V. Ignatov: *Steel USSR*, **5** (1975), 292.
- 7) M. Geerdes, R. Chaigneau, I. Kurunov, O. Lingardi and J. Ricketts: *Modern Blast Furnace Ironmaking*, IOS Press BV, Amsterdam, (2015), 218.
- 8) L. Lu, J. Pan and D. Zhu: *Iron Ore*, ed. by L. Lu, Woodhead Publishing, Cambridge, UK, (2015), 475. <https://doi.org/10.1016/B978-1-78242-156-6.00016-2>
- 9) D. Fernández-González, I. Ruiz-Bustinza, J. Mochón, C. González-Gasca and L. F. Verdeja: *Miner. Process. Extr. Metall. Rev.*, **38** (2017), 238. <https://doi.org/10.1080/08827508.2017.1288118>
- 10) K. Heinänen: Ph.D. thesis, University of Helsinki, (1993) 114.
- 11) R. Muroa, T. Harano, M. Kimura and I.-H. Jung: *ISIJ Int.*, **58** (2018), 259. <https://doi.org/10.2355/isijinternational.ISIJINT-2017-459>
- 12) K. Higuchi, M. Naito, M. Nakano and Y. Takamoto: *ISIJ Int.*, **44** (2004), 2057. <https://doi.org/10.2355/isijinternational.44.2057>
- 13) J. Mochón, A. Cores, Í. Ruiz-Bustinza, L. F. Verdeja, J. I. Robla and F. García-Carcedo: *Dyna*, **81** (2014), 168. <http://doi.org/10.15446/dyna.v81n183.41568>
- 14) W. Wang, X.-H. Chen, R.-S. Xu, J. Li, W.-J. Shen and S.-P. Wang: *J. Iron Steel Res. Int.*, **27** (2020), 367. <https://doi.org/10.1007/s42243-020-00374-4>
- 15) M. Pettersson, P. Sikström and V. Ritz: 5th Int. Conf. on Process Development in Iron and Steelmaking - SCANMET V, Swerea MEFOS, Luleå, (2016), 54.
- 16) A. Cores, A. Babich, M. Muñiz, S. Ferreira and J. Mochon: *ISIJ Int.*, **50** (2010), 1089. <https://doi.org/10.2355/isijinternational.50.1089>
- 17) M. Iljana, A. Kemppainen, T. Paananen, O. Mattila, E.-P. Heikkinen and T. Fabritius: *ISIJ Int.*, **56** (2016), 1705. <https://doi.org/10.2355/isijinternational.ISIJINT-2016-117>
- 18) T. Honeyands, J. Manuel, L. Matthews, D. O'Dea, D. Pinson, J. Leedham, G. Zhang, H. Li, B. Monaghan, X. Liu, E. Donskoi, N. A. S. Webster and M. I. Pownceby: *Minerals*, **9** (2019), 333. <https://doi.org/10.3390/min9060333>
- 19) M. I. Pownceby, N. A. S. Webster, J. R. Manuel and N. Ware: *Miner. Process. Extr. Metall.*, **125** (2016), 140. <https://doi.org/10.1080/03719553.2016.1153276>
- 20) T. Umadevi, K. Nelson, P. C. Mahapatra, M. Prabhu and M. Ranjan: *Ironmaking Steelmaking*, **36** (2009), 515. <https://doi.org/10.1080/08827508.2009.10800000>

- org/10.1179/174328109X445741
- 21) Z. Yan, J. Zhang, Z. Liu, X. Yuan, B. Gao and H. Zhang: 7th European Coke and Ironmaking Congr., ECIC 2016, ASMET, Leoben, (2016), 516.
  - 22) L. Lu, R. J. Holmes and J. R. Manuel: *ISIJ Int.*, **47** (2007), 349. <https://doi.org/10.2355/isijinternational.47.349>
  - 23) C. Chen, L. Zhang, L. Lu and S. Sun: *ISIJ Int.*, **50** (2010), 1523. <https://doi.org/10.2355/isijinternational.50.1523>
  - 24) H. B. Lungen, J. Noldin and P. Schmöle: *Stahl Eisen (Steel Iron)*, **135** (2015), 135 (in German).
  - 25) P. Schmöle: 7th European Coke and Ironmaking Congr., ECIC 2016, ASMET, Leoben, (2016), 3.
  - 26) P. Warren and D. Fisher: 7th European Coke and Ironmaking Congr., ECIC 2016, ASMET, Leoben, (2016), 3.
  - 27) R. Mežibrický, M. Fröhlichová, R. Findorák and V. S. Goettgens: *Minerals*, **9** (2019), 128. <https://doi.org/10.3390/min9020128>
  - 28) E. Donskoi, A. Poliakov, K. Vining and S. Hapugoda: 7th European Coke and Ironmaking Congr., ECIC 2016, ASMET, Leoben, (2016), 505.
  - 29) M. Zhang and M. Andrade: Characterization of Minerals, Metals, and Materials 2020, The Minerals, Metals & Materials Series, eds. by J. Li et al., Springer, Cham, (2020), 3. [https://doi.org/10.1007/978-3-030-36628-5\\_1](https://doi.org/10.1007/978-3-030-36628-5_1)
  - 30) B. Kain-Bückner, H. Mali, S. Schadler and E. Schuster: 7th European Coke and Ironmaking Congr., ECIC 2016, ASMET, Leoben, (2016), 534.
  - 31) B. Cai, T. Watanabe, C. Kamijo, M. Susa and M. Hayashi: *ISIJ Int.*, **58** (2018), 642. <https://doi.org/10.2355/isijinternational.ISIJINT-2017-552>
  - 32) L. Hsieh and J. A. Whiteman: *ISIJ Int.*, **29** (1989), 24. <https://doi.org/10.2355/isijinternational.29.24>
  - 33) L. Hsieh and J. A. Whiteman: *ISIJ Int.*, **29** (1989), 625. <https://doi.org/10.2355/isijinternational.29.625>
  - 34) L. Hsieh and J. A. Whiteman: *ISIJ Int.*, **33** (1993), 462. <https://doi.org/10.2355/isijinternational.33.462>
  - 35) R. Mežibrický, M. Fröhlichová and A. Mašlejová: *Arch. Metall. Mater.*, **60** (2015), 2955. <https://doi.org/10.1515/amm-2015-0472>
  - 36) H. Guo, B. Su, Z. Bai, J. Zhang, X. Li and F. Liu: *ISIJ Int.*, **54** (2014), 1222. <https://doi.org/10.2355/isijinternational.54.1222>
  - 37) X. Lv, C. Bai, G. Qiu, S. Zhang and R. Shi: *ISIJ Int.*, **49** (2009), 703. <https://doi.org/10.2355/isijinternational.49.703>
  - 38) Z. Xiao, L. Chen, Y. Yang, X. Li and M. Barati: *ISIJ Int.*, **57** (2017), 795. <https://doi.org/10.2355/isijinternational.ISIJINT-2016-688>
  - 39) A. Mašlejová, M. Fröhlichová, M. Černík, P. Vlašič and D. Ivanišič: *Acta Metall. Slovaca Conf.*, **4** (2014), 74. <http://doi.org/10.12776/amsc.v4i0.225>
  - 40) E. da Costa and J. P. Coheur: *Ironmaking Steelmaking*, **22** (1995), 223.
  - 41) L. Hsieh: *ISIJ Int.*, **45** (2005), 551. <https://doi.org/10.2355/isijinternational.45.551>
  - 42) N. V. Y. Scarlett, M. I. Pownceby, I. C. Madsen and A. N. Christensen: *Metall. Mater. Trans. B*, **35** (2004), 929. <https://doi.org/10.1007/s11663-004-0087-4>
  - 43) I. Tonžetić and A. Dippenaar: *Miner. Eng.*, **24** (2011), 1258. <https://doi.org/10.1016/j.mineng.2011.04.012>
  - 44) N. A. S. Webster, J. G. Churchill, F. Tufaile, M. I. Pownceby, J. R. Manuel and J. A. Kimpton: *ISIJ Int.*, **56** (2016), 1715. <https://doi.org/10.2355/isijinternational.ISIJINT-2016-162>
  - 45) J. Hancart: Ph.D. thesis, University of Liège, (1964), 158, [https://explore.lib.uliege.be/permalink/32ULG\\_INST/1iujq0/alma990000012300502321](https://explore.lib.uliege.be/permalink/32ULG_INST/1iujq0/alma990000012300502321), (accessed 2020-04-07) (in French).
  - 46) J. Hancart, V. Leroy and A. Bragard: *CNRM Metall. Rep.*, **DS 24/67** (1967), 3.
  - 47) C. Chen, L. Lu and K. Jiao: *Minerals*, **9** (2019), 361. <https://doi.org/10.3390/min9060361>
  - 48) W. G. Mumme, J. M. F. Clout and R. W. Gable: *Neues Jahrb. Mineral. Abh. (J. Min. Geochem.)*, **173** (1998), 93.
  - 49) A. Korytseva, N. A. S. Webster, M. I. Pownceby and A. Navrotsky: *J. Am. Ceram. Soc.*, **100** (2017), 3646. <https://doi.org/10.1111/jace.14857>
  - 50) W. G. Mumme: *Neues Jahrb. Mineral. Abh. (J. Min. Geochem.)*, **178** (2003), 307. <https://doi.org/10.1127/0077-7757/2003/0178-0307>
  - 51) K. Sugiyama, A. Monkawa and T. Sugiyama: *ISIJ Int.*, **45** (2005), 560. <https://doi.org/10.2355/isijinternational.45.560>
  - 52) A. Tazuddin, H. N. Aiyer and A. Chatterjee: *Calphad*, **60** (2018), 116. <https://doi.org/10.1016/j.calphad.2017.12.003>
  - 53) E. Jak, S. Degterov, P. C. Hayes and A. D. Pelton: *Fuel*, **77** (1998), 77. [https://doi.org/10.1016/S0016-2361\(97\)00137-3](https://doi.org/10.1016/S0016-2361(97)00137-3)
  - 54) R. H. Davies, A. T. Dinsdale, J. A. Gisby, J. A. J. Robinson and S. M. Martin: *Calphad*, **26** (2002), 229. [https://doi.org/10.1016/S0364-5916\(02\)00036-6](https://doi.org/10.1016/S0364-5916(02)00036-6)
  - 55) I.-H. Jung, S. A. Deckerov and A. D. Pelton: *Metall. Mater. Trans. B*, **35** (2004), 877. <https://doi.org/10.1007/s11663-004-0082-9>
  - 56) H. Lukas, S. G. Fries and B. Sundman: Computational Thermodynamics, The Calphad Method, Cambridge University Press, Cambridge, UK, (2007), 313.
  - 57) J. Ågren: *Curr. Opin. Solid State Mater. Sci.*, **1** (1996), 355. [https://doi.org/10.1016/S1359-0286\(96\)80025-8](https://doi.org/10.1016/S1359-0286(96)80025-8)
  - 58) Slag Atlas, ed. by Verein Deutscher Eisenhüttenleute (VDEh), Verlag Stahleisen GmbH, Düsseldorf, (1995), 616.
  - 59) H. Ohta and H. Suito: *ISIJ Int.*, **36** (1996), 983. <https://doi.org/10.2355/isijinternational.36.983>
  - 60) M. I. Pownceby, J. M. F. Clout and M. J. Fisher-White: *Miner. Process. Extr. Metall.*, **107** (1998), 1.
  - 61) M. I. Pownceby and J. M. F. Clout: *Miner. Process. Extr. Metall.*, **109** (2000), 36. <https://doi.org/10.1179/mpm.2000.109.1.36>
  - 62) H. Kimura, S. Endo, K. Yajima and F. Tsukihashi: *ISIJ Int.*, **44** (2004), 2040. <https://doi.org/10.2355/isijinternational.44.2040>
  - 63) H. M. Henaio, F. Kongoli and K. Itagaki: *Mater. Trans.*, **46** (2005), 812. <https://doi.org/10.2320/matertrans.46.812>
  - 64) H. Matsuura, M. Kurashige, M. Naka and F. Tsukihashi: *ISIJ Int.*, **49** (2009), 1283. <https://doi.org/10.2355/isijinternational.49.1283>
  - 65) I. Shigaki, M. Sawada, O. Tsuchiya, K. Yoshioka and T. Takahashi: *Tetsu-to-Hagane*, **70** (1984), 2208 (in Japanese). <https://doi.org/10.2355/tetsutohagane1955.70.16.2208>
  - 66) S. Nikolic, P. C. Hayes and E. Jak: *Metall. Mater. Trans. B*, **39** (2008), 179. <https://doi.org/10.1007/s11663-008-9130-1>
  - 67) S. Nikolic, H. Henaio, P. C. Hayes and E. Jak: *Metall. Mater. Trans. B*, **39** (2008), 189. <https://doi.org/10.1007/s11663-008-9131-0>
  - 68) T. Hidayat, P. C. Hayes and E. Jak: *Metall. Mater. Trans. B*, **43** (2012), 14. <https://doi.org/10.1007/s11663-011-9569-3>
  - 69) S. Chen, E. Jak and P. C. Hayes: *ISIJ Int.*, **45** (2005), 791. <https://doi.org/10.2355/isijinternational.45.791>
  - 70) S. Chen, E. Jak and P. C. Hayes: *ISIJ Int.*, **45** (2005), 1095. <https://doi.org/10.2355/isijinternational.45.1095>
  - 71) X. Ma, G. Wang, S. Wu, J. Zhu and B. Zhao: *ISIJ Int.*, **55** (2015), 2310. <https://doi.org/10.2355/isijinternational.ISIJINT-2015-263>
  - 72) X. Ma, D. Zhang, Z. Zhao, T. Evans and B. Zhao: *ISIJ Int.*, **56** (2016), 513. <https://doi.org/10.2355/isijinternational.ISIJINT-2015-486>
  - 73) C. Sun, X. Liu, J. Li, X. Yin, S. Song and Q. Wang: *ISIJ Int.*, **57** (2017), 978. <https://doi.org/10.2355/isijinternational.ISIJINT-2016-235>
  - 74) J. Gran, Y. Wang and D. Sichen: *Calphad*, **35** (2011), 249. <https://doi.org/10.1016/j.calphad.2010.11.004>
  - 75) H. Kimura, T. Ogawa, M. Kakiki, A. Matsumoto and F. Tsukihashi: *ISIJ Int.*, **45** (2005), 506. <https://doi.org/10.2355/isijinternational.45.506>
  - 76) M. Hayashi, H. Tanaka, T. Watanabe and M. Susa: *ISIJ Int.*, **57** (2017), 2124. <https://doi.org/10.2355/isijinternational.ISIJINT-2017-305>
  - 77) Y. Katahira, T. Watanabe and M. Hayashi: *ISIJ Int.*, **55** (2015), 2090. <https://doi.org/10.2355/isijinternational.ISIJINT-2015-229>
  - 78) S. Chen, E. Jak and P. C. Hayes: *ISIJ Int.*, **45** (2005), 1101. <https://doi.org/10.2355/isijinternational.45.1101>
  - 79) K. Yajima, H. Matsuura and F. Tsukihashi: *ISIJ Int.*, **50** (2010), 191. <https://doi.org/10.2355/isijinternational.50.191>
  - 80) K. Jang, X. Ma, J. Zhu, H. Xu, G. Wang and B. Zhao: *ISIJ Int.*, **56** (2016), 967. <https://doi.org/10.2355/isijinternational.ISIJINT-2016-099>
  - 81) K. Jang, X. Ma, J. Zhu, H. Xu, G. Wang and B. Zhao: *ISIJ Int.*, **56** (2016), 1728. <https://doi.org/10.2355/isijinternational.ISIJINT-2016-342>
  - 82) S. A. Degterov, E. Jak, P. C. Hayes and A. D. Pelton: *Metall. Mater. Trans. B*, **32** (2001), 643. <https://doi.org/10.1007/s11663-001-0119-2>
  - 83) T. Hidayat, D. Shishin, E. Jak and S. A. Deckerov: *Calphad*, **48** (2015), 131. <https://doi.org/10.1016/j.calphad.2014.12.005>
  - 84) P. J. Spencer and O. Kubaschewski: *Calphad*, **2** (1978), 147. [https://doi.org/10.1016/0364-5916\(78\)90032-9](https://doi.org/10.1016/0364-5916(78)90032-9)
  - 85) B. Sundman: *J. Phase Equilib.*, **12** (1991), 127. <https://doi.org/10.1007/BF02645709>
  - 86) O. B. Fabricnaya and B. Sundman: *Geochim. Cosmochim. Acta*, **61** (1997), 4539. [https://doi.org/10.1016/S0016-7037\(97\)00256-1](https://doi.org/10.1016/S0016-7037(97)00256-1)
  - 87) A. D. Pelton and M. Blander: *Metall. Mater. Trans. B*, **17** (1986), 805. <https://doi.org/10.1007/BF02657144>
  - 88) P. Wu, G. Eriksson and A. D. Pelton: *J. Am. Ceram. Soc.*, **76** (1993), 2065. <https://doi.org/10.1111/j.1151-2916.1993.tb08334.x>
  - 89) P. Wu, G. Eriksson, A. D. Pelton and M. Blander: *ISIJ Int.*, **33** (1993), 26. <https://doi.org/10.2355/isijinternational.33.26>
  - 90) G. Eriksson, P. Wu and A. D. Pelton: *Calphad*, **17** (1993), 189. [https://doi.org/10.1016/0364-5916\(93\)90019-8](https://doi.org/10.1016/0364-5916(93)90019-8)
  - 91) J. R. Taylor and A. T. Dinsdale: *Calphad*, **14** (1990), 71. [https://doi.org/10.1016/0364-5916\(90\)90041-W](https://doi.org/10.1016/0364-5916(90)90041-W)
  - 92) M. Hillert, B. Sundman and X. Wang: *Metall. Mater. Trans. B*, **21** (1990), 303. <https://doi.org/10.1007/BF02664198>
  - 93) W. Huang, M. Hillert and X. Wang: *Metall. Mater. Trans. A*, **26** (1995), 2293. <https://doi.org/10.1007/BF02671244>
  - 94) Z. Jin and Y. Du: *Calphad*, **16** (1992), 33. [https://doi.org/10.1016/0364-5916\(92\)90035-V](https://doi.org/10.1016/0364-5916(92)90035-V)
  - 95) M. Blander and A. D. Pelton: *Geochim. Cosmochim. Acta*, **51** (1987), 85. [https://doi.org/10.1016/0016-7037\(87\)90009-3](https://doi.org/10.1016/0016-7037(87)90009-3)
  - 96) G. Eriksson and A. D. Pelton: *Metall. Mater. Trans. B*, **24** (1993), 807.

- <https://doi.org/10.1007/BF02663141>
- 97) L. Zhang, S. Sun and S. Jahanshahi: *J. Phase Equilib. Diffus.*, **28** (2007), 121. <https://doi.org/10.1007/s11669-006-9002-9>
  - 98) H. Mao, M. Selleby and B. Sundman: *Calphad*, **28** (2004), 307. <https://doi.org/10.1016/j.calphad.2004.09.001>
  - 99) B. Hallstedt: *J. Am. Ceram. Soc.*, **73** (1990), 15. <https://doi.org/10.1111/j.1151-2916.1990.tb05083.x>
  - 100) T. Zienert and O. Fabrichnaya: *Calphad*, **40** (2013), 1. <https://doi.org/10.1016/j.calphad.2012.10.001>
  - 101) B. Hallstedt: *J. Am. Ceram. Soc.*, **75** (1992), 1497. <https://doi.org/10.1111/j.1151-2916.1992.tb04216.x>
  - 102) I.-H. Jung, S. A. Deckerov and A. D. Pelton: *J. Phase Equilib. Diffus.*, **25** (2004), 329. <https://doi.org/10.1007/s11669-004-0151-4>
  - 103) M. Hillert, M. Selleby and B. Sundman: *Metall. Trans. A*, **21** (1990), 2759. <https://doi.org/10.1007/BF02646071>
  - 104) T. Hidayat, D. Shishin, S. A. Deckerov and E. Jak: *Metall. Mater. Trans. B*, **47** (2016), 256. <https://doi.org/10.1007/s11663-015-0501-0>
  - 105) T. Hidayat, D. Shishin, S. A. Deckerov and E. Jak: *J. Phase Equilib. Diffus.*, **38** (2017), 477. <https://doi.org/10.1007/s11669-017-0535-x>
  - 106) I.-H. Jung, S. A. Deckerov and A. D. Pelton: *J. Phys. Chem. Solids*, **65** (2004), 1683. <https://doi.org/10.1016/j.jpcs.2004.04.005>
  - 107) L. Dreval, T. Zienert and O. Fabrichnaya: *J. Alloy. Compd.*, **657** (2016), 192. <https://doi.org/10.1016/j.jallcom.2015.10.017>
  - 108) V. Prostavkova, D. Shishin, M. Shevchenko and E. Jak: *Calphad*, **67** (2019), 101680. <https://doi.org/10.1016/j.calphad.2019.101680>
  - 109) B. Hallstedt, M. Hillert, M. Selleby and B. Sundman: *Calphad*, **18** (1994), 31. [https://doi.org/10.1016/0364-5916\(94\)90005-1](https://doi.org/10.1016/0364-5916(94)90005-1)
  - 110) M. Selleby: *Metall. Mater. Trans. B*, **28** (1997), 577. <https://doi.org/10.1007/s11663-997-0030-6>
  - 111) S. K. Saxena: *Geochim. Cosmochim. Acta*, **60** (1996), 2379. [https://doi.org/10.1016/0016-7037\(96\)00096-8](https://doi.org/10.1016/0016-7037(96)00096-8)
  - 112) I.-H. Jung, S. A. Deckerov and A. D. Pelton: *J. Eur. Ceram. Soc.*, **25** (2005), 313. <https://doi.org/10.1016/j.jeurceramsoc.2004.02.012>
  - 113) C. Chen, L. Zhang, L. Lu and S. Sun: *ISIJ Int.*, **50** (2010), 1523. <https://doi.org/10.2355/isijinternational.50.1523>
  - 114) T. Hidayat, D. Shishin, S. A. Deckerov and E. Jak: *Calphad*, **56** (2017), 58. <https://doi.org/10.1016/j.calphad.2016.11.009>
  - 115) O. B. Fabrichnaya: *Calphad*, **24** (2000), 113. [http://doi.org/10.1016/S0364-5916\(00\)00018-3](http://doi.org/10.1016/S0364-5916(00)00018-3)
  - 116) O. Fabrichnaya: *Calphad*, **22** (1998), 85. [https://doi.org/10.1016/S0364-5916\(98\)00016-9](https://doi.org/10.1016/S0364-5916(98)00016-9)
  - 117) S. A. Deckerov, I.-H. Jung and A. D. Pelton: *J. Am. Ceram. Soc.*, **85** (2002), 2903. <https://doi.org/10.1111/j.1151-2916.2002.tb00554.x>
  - 118) E. Jak, B. Zhao and P. Hayes: Proc. 6th Int. Conf. on Molten Slags, Fluxes and Salts, North-Holland, Amsterdam, (2001), 1.
  - 119) J.-O. Andersson, T. Helander, L. Höglund, P. Shi and B. Sundman: *Calphad*, **26** (2002), 273. [https://doi.org/10.1016/S0364-5916\(02\)00037-8](https://doi.org/10.1016/S0364-5916(02)00037-8)
  - 120) T. I. Barry, A. T. Dinsdale and J. A. Gisby: *JOM*, **45** (1993), 32. <https://doi.org/10.1007/BF03223284>
  - 121) S. A. Deckerov, I.-H. Jung, E. Jak, Y.-B. Kang, P. C. Hayes and A. D. Pelton: Proc. 7th Int. Conf. on Molten Slags, Fluxes and Salts, The South African Institute of Mining and Metallurgy, Johannesburg, (2004), 839.
  - 122) F. Kongoli and A. Yazawa: *Metall. Mater. Trans. B*, **32** (2001), 583. <https://doi.org/10.1007/s11663-001-0114-7>
  - 123) H. Gaye, P. V. Riboud and J. Welfringer: *Ironmaking Steelmaking*, **15** (1988), 319.
  - 124) J. Lehmann, N. Bontems, M. Simonnet, P. Gardin and L. Zhang: Proc. 8th Int. Conf. on Molten Slags, Fluxes and Salts, Gecamin, Santiago, (2009), 353.
  - 125) J. Lehmann, N. Bontems, M. Simonnet, P. Gardin and L. Zhang: *Steel Res. Int.*, **81** (2010), 772. <https://doi.org/10.1002/srin.201000056>
  - 126) J. Lehmann and L. Zhang: *Steel Res. Int.*, **81** (2010), 875. <https://doi.org/10.1002/srin.201000137>
  - 127) L. Zhang, S. Jahanshahi, S. Sun, C. Chen, B. Bourke, S. Wright and M. Somerville: *JOM*, **54** (2002), 51. <https://doi.org/10.1007/BF02709751>
  - 128) S. Jahanshahi, S. Sun and L. Zhang: *J. South. Afr. Inst. Min. Metall.*, **104** (2004), 529.
  - 129) C. W. Bale, P. Chartrand, S. A. Deckerov, G. Eriksson, K. Hack, R. Ben Mahfoud, J. Melançon, A. D. Pelton and S. Petersen: *Calphad*, **26** (2002), 189. [https://doi.org/10.1016/S0364-5916\(02\)00035-4](https://doi.org/10.1016/S0364-5916(02)00035-4)
  - 130) C. W. Bale, E. Bélisle, P. Chartrand, S. A. Deckerov, G. Eriksson, K. Hack, I.-H. Jung, Y.-B. Kang, J. Melançon, A. D. Pelton, C. Robelin and S. Petersen: *Calphad*, **33** (2009), 295. <https://doi.org/10.1016/j.calphad.2008.09.009>
  - 131) C. W. Bale, E. Bélisle, P. Chartrand, S. A. Deckerov, G. Eriksson, A. E. Gheribi, K. Hack, I.-H. Jung, Y.-B. Kang, J. Melançon, A. D. Pelton, S. Petersen, C. Robelin, J. Sangster, P. Spencer and M.-A. Van Ende: *Calphad*, **54** (2016), 35. <https://doi.org/10.1016/j.calphad.2016.05.002>
  - 132) J. Gisby, P. Taskinen, J. Pihlasalo, Z. Li, M. Tyrer, J. Pearce, K. Avarmaa, P. Björklund, H. Davies, M. Korpi, S. Martin, L. Pesonen and J. Robinson: *Metall. Mater. Trans. B*, **48** (2017), 91. <https://doi.org/10.1007/s11663-016-0811-x>
  - 133) H. Gaye, J. Lehmann, P. Rocabois and F. Ruby-Meyer: *High Temp. Mater. Process.*, **20** (2001), 285. <https://doi.org/10.1515/HTMP.2001.20.3-4.285>
  - 134) I.-H. Jung: *Calphad*, **34** (2010), 332. <https://doi.org/10.1016/j.calphad.2010.06.003>
  - 135) S. Nicol, J. Chen, M. I. Pownceby and N. A. S. Webster: *ISIJ Int.*, **58** (2018), 2157. <https://doi.org/10.2355/isijinternational.ISIJINT-2018-203>
  - 136) A. D. Pelton, S. A. Deckerov, G. Eriksson, C. Robelin and Y. Dessureault: *Metall. Mater. Trans. B*, **31** (2000), 651. <https://doi.org/10.1007/s11663-000-0103-2>
  - 137) A. D. Pelton and P. Chartrand: *Metall. Mater. Trans. A*, **32** (2001), 1355. <https://doi.org/10.1007/s11661-001-0226-3>
  - 138) P. Chartrand and A. D. Pelton: *Metall. Mater. Trans. A*, **32** (2001), 1397. <https://doi.org/10.1007/s11661-001-0229-0>
  - 139) A. D. Pelton, P. Chartrand and G. Eriksson: *Metall. Mater. Trans. A*, **32** (2001), 1409. <https://doi.org/10.1007/s11661-001-0230-7>
  - 140) M. L. Kapoor and M. G. Froberg: Chemical Metallurgy of Iron and Steel: Proc. Int. Symp. on Metallurgical Chemistry - Applications in Ferrous Metallurgy, Iron and Steel Institute, London, (1973), 17.
  - 141) H. Gaye and J. Welfringer: Proc. 2nd Int. Symp. on Metallurgical Slags and Fluxes, The Metallurgical Society of AIME, Warrendale, (1984), 357.
  - 142) M. Hillert, B. Jansson, B. Sundman and J. Ågren: *Metall. Trans. A*, **16** (1985), 261. <https://doi.org/10.1007/BF02815307>
  - 143) M. Hillert: *J. Alloy. Compd.*, **320** (2001), 161. [https://doi.org/10.1016/S0925-8388\(00\)01481-X](https://doi.org/10.1016/S0925-8388(00)01481-X)
  - 144) T. I. Barry, A. T. Dinsdale, J. A. Gisby, B. Hallstedt, M. Hillert, B. Jansson, S. Jonsson, B. Sundman and J. R. Taylor: *J. Phase Equilib.*, **13** (1992), 459. <https://doi.org/10.1007/BF02665760>
  - 145) M. Hillert, L. Kjellqvist, H. Mao, M. Selleby and B. Sundman: *Calphad*, **33** (2009), 227. <https://doi.org/10.1016/j.calphad.2008.05.006>
  - 146) E. Moosavi-Khoonsari and I.-H. Jung: *J. Eur. Ceram. Soc.*, **37** (2017), 787. <https://doi.org/10.1016/j.jeurceramsoc.2016.06.021>
  - 147) T. Jantzen, K. Hack, E. Yazhenskikh and M. Müller: *Calphad*, **62** (2018), 187. <https://doi.org/10.1016/j.calphad.2018.05.009>
  - 148) H. Suito and R. Inoue: *Trans. Iron Steel Inst. Jpn.*, **24** (1984), 301. <https://doi.org/10.2355/isijinternational.1966.24.301>
  - 149) S. C. Duan, X. L. Guo, H. J. Guo and J. Guo: *Ironmaking Steelmaking*, **44** (2017), 168. <https://doi.org/10.1080/03019233.2016.1198859>
  - 150) B. Zhao, E. Jak and P. C. Hayes: *ISIJ Int.*, **46** (2006), 1594. <https://doi.org/10.2355/isijinternational.46.1594>
  - 151) C. Zhu, G. Li, Z. Chen, G. Ma and J. Liu: *ISIJ Int.*, **48** (2008), 123. <https://doi.org/10.2355/isijinternational.48.123>
  - 152) A. S. Sunkar and K. Morita: *ISIJ Int.*, **49** (2009), 1649. <https://doi.org/10.2355/isijinternational.49.1649>
  - 153) T. R. C. Patrick and M. I. Pownceby: *Metall. Mater. Trans. B*, **33** (2002), 79. <https://doi.org/10.1007/s11663-002-0088-0>
  - 154) M. I. Pownceby and J. M. F. Clout: *Miner. Process. Extr. Metall.*, **112** (2003), 44. <https://doi.org/10.1179/037195503225011402>
  - 155) M. I. Pownceby and T. R. C. Patrick: *Eur. J. Mineral.*, **12** (2000), 455. <https://doi.org/10.1127/0935-1221/2000/0012-0455>
  - 156) K. Inoue and T. Ikeda: *Tetsu-to-Hagané*, **68** (1982), 2190 (in Japanese). [https://doi.org/10.2355/tetsutohagane1955.68.15\\_2190](https://doi.org/10.2355/tetsutohagane1955.68.15_2190)
  - 157) P. R. Dawson, J. Ostwald and K. M. Hayes: *BHP Tech. Bull.*, **27** (1983), 47.
  - 158) N. A. S. Webster, M. I. Pownceby, I. C. Madsen and J. A. Kimpton: *Metall. Mater. Trans. B*, **43** (2012), 1344. <https://doi.org/10.1007/s11663-012-9740-5>
  - 159) N. A. S. Webster, M. I. Pownceby, I. C. Madsen and J. A. Kimpton: *ISIJ Int.*, **53** (2013), 774. <https://doi.org/10.2355/isijinternational.53.774>
  - 160) N. A. S. Webster, M. I. Pownceby, I. C. Madsen, A. J. Studer, J. R. Manuel and J. A. Kimpton: *Metall. Mater. Trans. B*, **45** (2014), 2097. <https://doi.org/10.1007/s11663-014-0137-5>
  - 161) N. A. S. Webster, M. I. Pownceby, R. Pattel, J. R. Manuel and J. A. Kimpton: *ISIJ Int.*, **59** (2019), 1007. <https://doi.org/10.2355/isijinternational.ISIJINT-2018-701>
  - 162) N. A. S. Webster, M. I. Pownceby, R. Pattel, J. R. Manuel and J. A. Kimpton: *ISIJ Int.*, **59** (2019), 263. <https://doi.org/10.2355/isijinternational.ISIJINT-2018-573>
  - 163) M. Iljana: Ph.D. thesis, University of Oulu, (2017), 104. <http://urn.fi/urn:isbn:9789526215709>, (accessed 2019-04-10).
  - 164) M. Iljana, A. Kemppainen, E.-P. Heikkinen, T. Fabritius, T. Paananen and O. Mattila: European Steel Technology and Application Days - METEC & 2nd ESTAD, TEMA Technologie Marketing AG, Aachen, (2015), 1.